

AD-A141 095

THE TRANSIENT GRAVITY WAVE CRITICAL LAYER(U) PHYSICAL  
DYNAMICS INC BELLEVUE WA T J DUNKERTON 09 APR 84

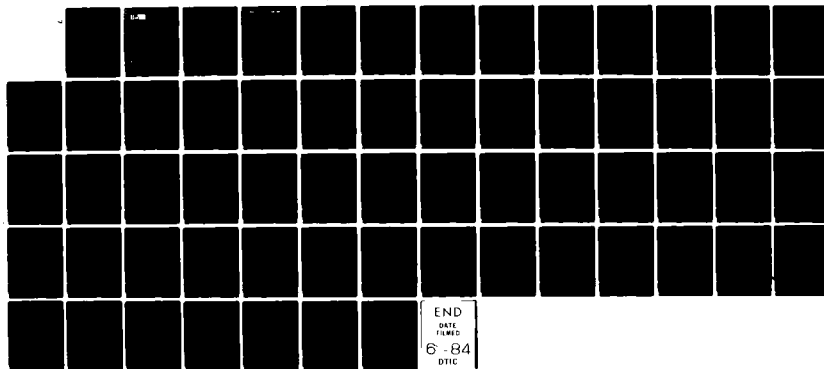
1/1

PD-NW-84-310R AFOSR-TR-84-0334 F49620-83-C-0061

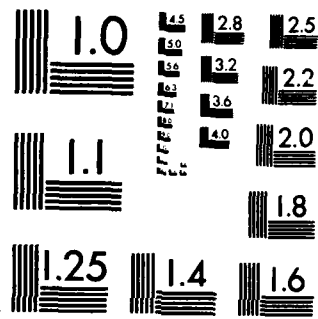
F/G 8/5

NL

UNCLASSIFIED



END  
DATE  
FILED  
6-84  
DTC



MICROCOPY RESOLUTION TEST CHART  
NATIONAL BUREAU OF STANDARDS-1963-A

APR 10 1984



**physical dynamics, inc.**

AD-A141 095

PD-NW-84-310R

THE TRANSIENT GRAVITY WAVE CRITICAL LAYER

Timothy J. Dunkerton  
Physical Dynamics, Inc.  
300 120th Ave. NE, Bldg. 7  
Bellevue, WA 98005

9 April 1984

Annual Report  
Contract #F49620-83-C-0061

Prepared for  
AIR FORCE OFFICE OF SCIENTIFIC RESEARCH  
Bolling AFB  
Washington, DC 20332



Approved for public release;  
distribution unlimited.

84 05 15 234

PD-NW-84-310R

THE TRANSIENT GRAVITY WAVE CRITICAL LAYER

Timothy J. Dunkerton  
Physical Dynamics, Inc.  
300 120th Ave. NE, Bldg. 7  
Bellevue, WA 98005

9 April 1984

Annual Report  
Contract #F49620-83-C-0061

Prepared for  
AIR FORCE OFFICE OF SCIENTIFIC RESEARCH  
Bolling AFB  
Washington, DC 20332

AIR FORCE OFFICE OF SCIENTIFIC RESEARCH (AFOSR)  
NOTICE OF TRANSMISSION TO DTIC  
This technical report has been reviewed and is  
approved for public release. The IAW AFR 190-12.  
Distribution is unlimited.  
MATTHEW J. KERPER  
Chief, Technical Information Division

UNCLASSIFIED

SECURITY CLASSIFICATION OF THIS PAGE (When Data Entered)

REPORT DOCUMENTATION PAGE		READ INSTRUCTIONS BEFORE COMPLETING FORM
1. REPORT NUMBER <b>AFOSR-TR- 84-0334</b>	2. GOVT ACCESSION NO. <b>AM1095</b>	3. SUPPLEMENTARY CATALOG NUMBER
4. TITLE (and Subtitle) <b>THE TRANSIENT GRAVITY WAVE CRITICAL LAYER</b>	5. TYPE OF REPORT & PERIOD COVERED <b>Annual Report covering 10 Feb 83 - 10 Feb 84</b>	
7. AUTHOR(s) <b>Timothy J. Dunkerton</b>	6. PERFORMING ORG. REPORT NUMBER <b>PD-NW-84-310R</b>	
9. PERFORMING ORGANIZATION NAME AND ADDRESS <b>Physical Dynamics, Inc. 300 120th Ave. NE, Bldg 7, Suite 220 Bellevue, WA 98005</b>	10. PROGRAM ELEMENT, PROJECT, TASK AREA & WORK UNIT NUMBERS <b>L61102F 2310/A1</b>	
11. CONTROLLING OFFICE NAME AND ADDRESS <b>Air Force Office of Scientific Research / NC Bolling AFB Washington, DC 20332</b>	12. REPORT DATE <b>9 April 1984</b>	
14. MONITORING AGENCY NAME & ADDRESS (if different from Controlling Office)	13. NUMBER OF PAGES <b>601</b>	
16. DISTRIBUTION STATEMENT (of this Report)	15. SECURITY CLASS. (of this report) <b>UNCLASSIFIED</b>	
17. DISTRIBUTION STATEMENT (of the abstract entered in Block 20, if different from Report) <b>Approved for public release, distribution unlimited</b>	18. SUPPLEMENTARY NOTES	
19. KEY WORDS (Continue on reverse side if necessary and identify by block number) <b>Gravity waves Critical layers</b>	20. ABSTRACT (Continue on reverse side if necessary and identify by block number) <b>Numerical simulations of gravity wave, critical layer interactions are presented, which confirm theoretical predictions of critical layer behavior and explain important features of gravity wave observations in the atmosphere, including momentum deposition and convective wavebreaking.</b>	

DD FORM 1 JAN 73 1473

EDITION OF 1 NOV 65 IS OBSOLETE

UNCLASSIFIED  
SECURITY CLASSIFICATION OF THIS PAGE (When Data Entered)

## Summary

The research supported under Contract F49620-83-C-0061 represents an effort to understand, both theoretically and observationally, the role of gravity waves in the general circulation of the atmosphere. Gravity waves redistribute momentum and trace species through the atmosphere, operating at all scales of motion from equatorial planetary waves down to the mesoscale. Our current research examines the propagation and nonlinear breakdown of these waves, as well as the ensuing redistributive effects.

In this report, numerical simulations are described which reveal how a transient gravity wave packet behaves when encountering its critical layer, where phase speed equals mean flow speed. The critical layer becomes a focus of wavebreaking, where momentum is deposited and convective turbulence occurs. The numerical solutions afford important checks on theoretical predictions of critical layer behavior, as well as explaining the observational evidence obtained from the MST radar. Importantly, the redistributive effects at the critical layer are also seen in more general circumstances in which gravity wavebreaking is attributable to the mean density profile rather than shear.

The inviscid gravity wave critical layer is inherently turbulent since overturning rapidly develops in the potential temperature field. Negative local Richardson numbers ( $Ri$ ) are contemporaneous with the development of the internal shock in the monochromatic wave events, are coincident with Lagrangian zonal perturbation velocities exceeding the intrinsic phase speed, and occur very soon after the appearance of regions with  $Ri < 1/4$ . To account for convective wavebreaking a simple, local turbulence parameterization is advanced, which is not based upon turbulent eddy diffusion. Instead, the total wave + mean flow profile, when required, is frictionally relaxed to a convectively neutral equilibrium which conserves potential temperature and total vorticity, analogous to the familiar "convective adjustment" procedure in general circulation models. Despite being a local adjustment within the wave, this turbulence parameterization seems to confirm the qualitative features predicted by Lindzen's (1981) global amplitude balance model in the relatively simple case studies presented here.

## Preface

Part of this research was performed in collaboration with Dr. David C. Fritts at the Geophysical Institute, University of Alaska. The author thanks Dr. Fritts for his mutual support and many helpful interactions, and for allowing the author to implement his numerical code in this study.

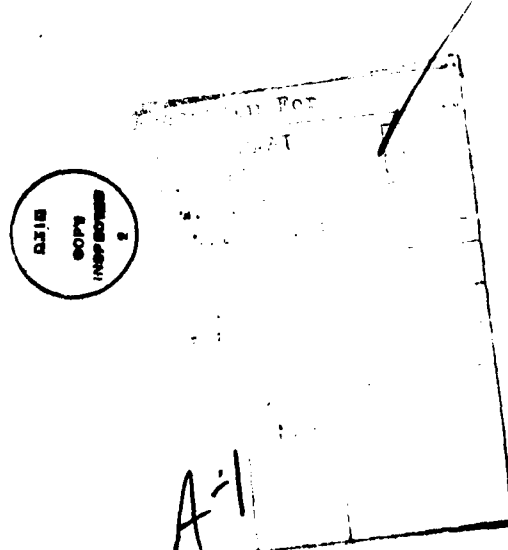


## TABLE OF CONTENTS

	<u>Page</u>
1. STATEMENT OF PROBLEM	1
a. Gravity waves in the atmosphere	1
b. Relevance of wavebreaking	1
c. Linear critical level	2
d. Deficiencies of linear theory	2
e. Research problems	5
f. Progress summary	5
2. THE SEMI-ANALYTIC MODEL OF GRAVITY WAVE, MEAN-FLOW INTERACTION	7
3. MODEL DISCUSSION	12
4. COMPARISON OF SEMI-ANALYTIC AND NUMERICAL SOLUTIONS	15
5. A LOCAL CONVECTIVE ADJUSTMENT PARAMETERIZATION	29
a. Earlier turbulent adjustment schemes	30
b. Convective adjustment	30
c. Relaxation to neutral equilibrium	32
6. IRREVERSIBLE ABSORPTION AND MEAN FLOW ACCELERATION AT THE CRITICAL LAYER	35
7. CONCLUSION	46
REFERENCES	47
PUBLICATION LIST	52

## LIST OF FIGURES

	<u>Page</u>
<b>Figure 1.</b> Semi-analytic saturated GDC solution for nondimensional wave action density and percent increase in phase speed for the case discussed in Section 2.	10
<b>Figure 2.</b> Zonal mean wind at $t=1000$ and $12000$ s. for Case I. (In this and the following figures $z_0$ is the domain height, 30 km.) Units: $ms^{-1}$ .	16
<b>Figure 3.</b> Perturbation zonal wind for Case I at (a) $t=4000$ s, and (b) $t = 8000$ s. Also shown are estimated intrinsic phase speeds (dashed line) and region of overturning (vertical bar at left). Units: $ms^{-1}$ .	17
<b>Figure 4.</b> Zonal mean wind for Case II at (a) $t=8000$ s, (b) $t=12000$ s, compared to the initial mean flow (dashed line) and saturated GDC solution (triangles). Units: $ms^{-1}$ .	19
<b>Figure 5.</b> Potential temperature fields $\theta(x,z)$ for Case II at (a) $t=6000$ s, (b) $t=7000$ s., (c) $t=8000$ s., and (d) $t=9000$ s. contour interval is .025 in nondimensional units normalized by $\bar{\theta}(0)$ .	22
<b>Figure 6.</b> Partial reflection from the internal shock in Case III at $t=22000$ s., (a) mean flow profile in $ms^{-1}$ ; (b) eddy kinetic energy showing reflected wave component below the critical layer.	26
<b>Figure 7.</b> Illustration of how a unique equilibrium potential temperature profile $\theta^E(z)$ is created from an unstable $\theta$ -column. The shaded regions represent equal areas (mass-weighted in general) thus conserving potential temperature. The equilibrium vorticity profile $n^E(z)$ is set equal to the average value of $n$ in the mixed region; outside this region, $\theta^E \equiv \theta$ and $n^E \equiv n$ .	33
<b>Figure 8.</b> Potential temperature fields $\theta(x,z)$ for Case II with convective adjustment; (a) $t=7000$ s., (b) $t=8000$ s., (c) $t=9000$ s., (d) $t=12000$ s.	36

	<u>Page</u>
Figure 9. Domain-integrated eddy kinetic energy for Case II with convective adjustment for the forced wave (#1) and its higher harmonics. Dashed line represents the unstable linear solution; arrow indicates onset of breaking.	40
Figure 10. Zonal mean wind at $t=12000$ s. for Case II with convective adjustment, compared to the initial mean flow (dashed line) and saturated GDC solution (triangles). Units: $ms^{-1}$ .	43

## I. STATEMENT OF PROBLEM

### a. Gravity waves in the atmosphere

Atmospheric gravity waves are increasingly being recognized and studied as an important dynamical mechanism by which horizontal momentum is transported upward over many scale heights, resulting in significant mean flow accelerations in the stratosphere, mesosphere, and lower thermosphere (Lindzen, 1981; Matsuno, 1982; Holton, 1982; Dunkerton, 1981, 1982a,b). The operational network of MST radars is beginning to provide important glimpses, here and there, of the magnitude and distribution of this momentum transport process (Balsley et al, 1980; Balsley and Gage, 1980; Vincent and Reid, 1983; Balsley et al, 1983). In the winter mesosphere in particular, gravity wave momentum deposition, or some other mechanism, seems required to balance the mean Coriolis torques driven by radiative cooling in the polar night (Leovy, 1964; Mahlman and Sinclair, 1979; Lindzen, 1981; Matsuno, 1982; Holton, 1982; Dunkerton, 1982a,b). Preliminary estimates of gravity wave momentum fluxes confirm their ability to retard the mean flow in this manner, although this of course does not exclude the possible role of other mechanisms such as the unstable breakdown and/or radiative decay of planetary scale waves (e.g. Lindzen and Schoeberl, 1982).

### b. Relevance of wavebreaking

Because transient, conservative waves have no permanent effect on the mean flow (Eliassen and Palm, 1960; Charney and Drazin, 1961; Andrews and McIntyre, 1976, 1978; Boyd, 1976; Dunkerton, 1980, 1981, 1982a), irreversible mixing and mean flow acceleration must ultimately be attributed to wave dissipation. For atmospheric gravity waves, the relevant dissipative process seems to involve their unstable breakdown via convective and/or dynamical instabilities (Lindzen, 1981; Holton, 1982; Weinstock, 1982; Fritts, 1982b; Dunkerton, 1982a; Lindzen and Forbes, 1983). In this paper, attention will be focused on the mean zonal wind accelerations due to wavebreaking; however, the simultaneous irreversible mixing is likely to be important for trace species concentrations in the middle atmosphere (M.R. Schoeberl, S. Solomon, personal communications, 1982).

### c. Linear critical level

The gravity wave excitation mechanisms have been studied extensively, and are thought to include shear instability (Davis and Peltier, 1979; Lalas and Einaudi, 1976; Lindzen and Rosenthal, 1976; Patnaik *et al*, 1976; McIntyre and Weissman, 1978; Fritts, 1979, 1982a), topography (Klemp and Lilly, 1978; Peltier and Clark, 1979; Blumen and Dietze, 1981; Durran and Klemp, 1982), and convection (Curry and Murty, 1974; Balachandran, 1980; Larsen *et al*, 1982). What happens to those propagating waves able to radiate large distances from their source regions, however, is less well understood. Until the last decade our understanding of atmospheric gravity wave propagation was built around classical linear wave theory. Propagating waves, if steady and conservative, do not accelerate the mean flow anywhere, except where

$$\bar{u} = c \quad (1.1)$$

the so-called "critical level", where the mean flow equals the horizontal wave phase speed (Eliassen and Palm, 1960). At this point the vertical group velocity of slowly-varying waves vanishes (Bretherton, 1966) and for finite  $Ri$  the wave is attenuated by the factor  $\exp 2\mu\pi$ , where

$$\mu = \sqrt{Ri - 1/4} \quad (1.2)$$

The singularity (1.1) implies, for example, an infinite momentum flux convergence at the steady-state critical level (Booker and Bretherton, 1967).

### d. Deficiencies of linear theory

In more recent years the Booker-Bretherton solution has been cross-examined by a number of theoreticians and experimentalists who have sought to determine to what extent this linear solution is relevant to geophysical critical layers. As a barrier to wave propagation their solution has stood the test of time quite well. Nevertheless, three possible shortcomings of the linear solution have been uncovered, having to do with the fact that Booker and Bretherton (1967) neglected convective wavebreaking, the quasi-linear mean flow modification, and wave, wave interactions.

First, if the critical level (1.1) is an absorbing barrier to wave propagation, then any incident wave packet in a conservative fluid will occupy a finite vertical domain bounded by the critical level. Now conservation of wave action integrated over the entire wave packet (Bretherton, 1966; Bretherton and Garrett, 1968) implies that local values of  $A$ , the wave action density -- which for a constant horizontal wavelength is related to the wave energy density  $E$  as

$$kA = \frac{E}{c-u} \quad (1.3)$$

-- increases indefinitely with time as wave action "piles up" beneath the initial critical level. This increase in  $A$  due to shear is of course analogous to the amplitude growth with height experienced by vertically-propagating waves in a compressible atmosphere (Dunkerton, 1981). But as noted by Lindzen (1981) and Dunkerton (1982a), when

$$kA = \frac{1}{2}(c-u) \quad (1.4)$$

for waves propagating in the direction of the mean flow, the wave is marginally stable to convection in the sense that at some point

$$\theta_z = \theta_z + \bar{\theta}'_z = 0 \quad (1.5)$$

within the wave,  $\theta$  being potential temperature. Because when  $\theta_z < 0$  the convective instabilities will have an initial growth rate

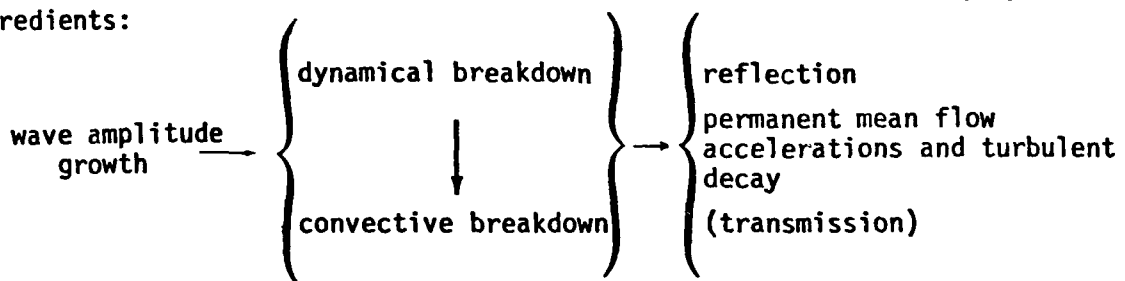
$$\omega_1^2 = 0 \left( g \frac{|\theta_z|}{\theta} \right) \quad (g = 9.8 \text{ ms}^{-2}) \quad (1.6)$$

which is large relative to the intrinsic frequency of the wave as the critical level is approached, convective breakdown of the wave is expected to occur (Thorpe, 1981; Koop, 1981).

Second, an upward propagating wave packet induces mean flow accelerations due to wave transience (Dunkerton, 1981 Fritts, 1982b). But on account of irreversible wavebreaking these transient accelerations will include a permanent component well below the initial critical level (Dunkerton, 1982a). This feature was observed several years ago in the numerical model of Jones

and Houghton (1971) but went unexplained until a quasi-linear theory was advanced by Grimshaw (1975), Dunkerton (1981, 1982a) and Coy (1984). Incidentally, this mean flow evolution does not require an initial critical level, since atmospheric compressibility also leads to wave growth as noted above. In either case there may be significant, permanent mean flow accelerations well below an initial critical level (1.1).

Third, the importance of wave, wave interactions has become the keynote in the recent advent of "nonlinear critical layer theory," and the discovery of nonlinear steady-state critical layers (Benney and Bergeron, 1969; Davis, 1969; Haberman, 1971; Beland, 1978; Warn and Warn, 1978; Maslowe, 1973, 1977). Although the transient development and hydrodynamic stability of these analytic solutions needs to be examined further, it must be admitted that (1.5) is not a necessary condition for instability of the wave, nor is the K-H condition  $Ri < 1/4$ . Resonant triad interactions, for example, might cause a dynamical "breakdown" of the incident wave (McComas and Bretherton, 1977; Weinstock, 1982; Lindzen and Forbes, 1983). Once wave, wave interactions become significant it is no longer obvious that the critical layer is simply an absorber of the incident wave; it may act as a reflector (Brown and Stewartson, 1980; also evident in Thorpe, 1981) or, with perhaps considerably greater difficulty, allow some wave action to be transmitted. Thus a more general scenario of transient gravity wave critical layer interaction than that proposed by Booker and Bretherton (1967) would include the following ingredients:



It is expected that dynamical breakdown will ultimately lead to convective breakdown (e.g. Lindzen and Forbes, 1983). Also, allowance has been made for reflection and transmission caused by either dynamical or convective instability.

e. Research problems

This theoretical scenario is still somewhat tentative, having several unanswered questions associated with it. As already noted, it is uncertain whether convective instability will preclude formation of the nonlinear steady-state critical layer in the inviscid case (which, unfortunately, is difficult to examine experimentally). The occurrence of nonlinear reflection could, for example, significantly reduce the mean flow modification predicted by quasi-linear theory, although it will certainly not eliminate it. Irrespective of this, there are some outstanding questions regarding the accuracy of the quasi-linear solutions themselves and their dependence on the WKB approximation (see Dunkerton, 1981). Perhaps the most difficult question of all is whether or not there exist circumstances in which critical layer transmission is possible to a much greater extent than predicted by Booker and Bretherton (1967).

f. Progress summary

In an attempt to resolve some of these issues, and to stimulate further experimental work in this area, the author's research seeks to investigate the transient gravity wave critical layer interaction with the help of a deterministic numerical model developed by Fritts (1979; 1982b). In this annual report attention will be focused on two aspects of this problem. First, except for the pioneering work of Jones and Houghton (1971), the semi-analytic model of gravity wave, mean-flow interaction advanced by Grimshaw (1975), Dunkerton (1981, 1982a), and Coy (1984) (hereafter GDC) has not been tested numerically. The properties of this model are reviewed in Section 2, and after describing the numerical model in Section 3, the accuracy of the GDC solution method is examined numerically in Section 4.

Second, recognizing that inviscid gravity wave critical layers are convectively unstable, a successful attempt has been made to introduce a turbulence parameterization scheme which eliminates superadiabatic regions while conserving potential temperature and total vorticity. Turbulence parameterization in unstable gravity wave motion has been used by several previous authors, but what is unique about the convective adjustment scheme used here

is its computational efficiency and physical appeal, being designed with high Reynolds and high Rayleigh number flows specifically in mind and avoiding any reference to artificial eddy diffusion. This convective adjustment scheme is described in Section 5 and some preliminary results are presented in Section 6.

A discussion of the role of wave, wave interactions in gravity wave critical layer interaction is reserved for the coming year, in which the numerical simulations will also be generalized to include more complex flow profiles and forcings.

## 2. THE SEMI-ANALYTIC MODEL OF GRAVITY WAVE, MEAN-FLOW INTERACTION

When a single linear plane wave, or a set of such waves acting independently of one another, interact with the mean flow, with wave, wave interactions neglected, the model is said to be "quasi-linear". When in addition the waves are accurately described by the WKB approximation, i.e. if the wave amplitude and mean flow vary slowly over a vertical wavelength, the model waves are "quasi-linear and slowly-varying." The mathematical problem then reduces to a mean flow evolution equation together with a pair of equations for each wave, viz. a wave action conservation equation and a "conservation of wavenumber" equation. For two dimensional flow,

$$u_t + \frac{1}{\rho_0} \sum_i (\rho_0 \overline{u'_i w'_i})_z + \dots = 0 \quad (2.1)$$

where  $u'$  and  $w'$  are horizontal and vertical perturbation velocity and  $\rho_0 = \rho_s \exp -z/H$ , the basic state density. For each wave,

$$A_t + \frac{1}{\rho_0} (\rho_0 W_g A)_z = 0 \quad (2.2)$$

$$m_t + \omega_z = 0 \quad (2.3)$$

where  $W_g$  is the vertical group velocity,  $m$  is vertical wavenumber, and  $\omega$  is frequency relative to the ground. Grimshaw (1975) solved Eqs. (2.1-3) numerically for a single wave propagating towards its critical level. Dunkerton (1981, 1982a) obtained analytic solutions by reduction to a single equation

$$A_t + \frac{1}{\rho_0} \left[ \rho_0 W_g (\bar{u}_0, A) \right]_z = 0 \quad (2.4)$$

where  $\bar{u}_0$  is the initial mean flow when  $A = 0$ . The crucial approximation involves setting  $\omega = \text{constant}$  in (2.3). Kelvin's circulation theorem implies

$$\bar{u} = A + \bar{u}_0 \quad (2.5)$$

Recently, Coy (1984) has tested the accuracy of Dunkerton's (1981) approximation by numerically solving Eqs. (2.1-3) for a variety of initial profiles.

It turns out that the approximation is quite accurate in cases where an incident wave packet encounters a critical level within a few scale heights of its forcing level; in these cases the acceleration of wave frequency implied by (2.3) is largely suppressed by the presence of the critical level. On the other hand, with no initial mean flow, Dunkerton's (1981) approximation yields the correct level of wavebreaking, but fails to predict the twofold or more increase in  $\omega$  at the front of the wave packet even when the global saturation limit (1.4) is imposed (without which there seems to be no asymptotic limit to the attainable phase speeds and mean flow speeds at the leading edge of the wave packet).

The semi-analytic solutions calculated by the GDC method have at least five interesting features for wave packets of finite duration. First, as the wave group propagates vertically, insofar as the forcing remains steady, an equilibrated solution is traced out beginning at the level of forcing. In this region a small but temporary mean flow change has occurred (Dunkerton, 1981). Second the "radiating" solution in the wavefront region increases in amplitude with height, soon becoming convectively unstable in the sense that (1.5) is satisfied locally within the wave (Dunkerton, 1982a). Third, after a finite time a mean flow and wave action discontinuity develops between the equilibrated and radiating solutions due to the overlapping of characteristics. This "internal shock" descends gradually with time so as to conserve momentum (Dunkerton, 1982a). Fourth, if the wave forcing decreases abruptly, a second discontinuity, or "trailing shock", forms at the rear of the wave packet (Grimshaw, 1975; Dunkerton, 1982a). Fifth, the leading edge of the wave packet tends to separate from the lower solution due to its increasing vertical group velocity (Grimshaw, 1975; Coy, 1984). This effect, however, is largely suppressed when a critical level is encountered close to the forcing level.

To illustrate the GDC solution method, Eqs. (2.1-3) were solved on a finite difference grid with the equations written in nondimensional form following Dunkerton (1981): dimensionless height is scaled by  $H$ , dimensionless wave action, mean flow, and phase speed are scaled by the forced phase speed  $c(0)$ , and dimensionless time is scaled by  $NH/kc^2(0)$ , where  $N$  is the static

stability and  $k$  is zonal wavenumber. Fig. 1 displays the nondimensional wave action density  $A^*$  and percent increase in phase speed for the case

$$\bar{u}_0^* = 1.03 \tanh \frac{z^*-1.93}{.86} + 1.00 \quad (2.6a)$$

$$A^*(0) = .0092 \sin^4 \frac{\pi t}{14.2} \quad (t < 14.2) \quad (2.6b)$$

$$W_g^* = (c^* - \bar{u}^*)^2 \quad (2.6c)$$

corresponding to a numerical simulation performed during the course of this investigation. The initial critical level is at 1.93 scale heights. (For the numerical simulation corresponding to this solution, the scale height is 9.333 km,  $c(0) = 39 \text{ ms}^{-1}$ , and the time scale is 864 s.) The initial critical level acts as a complete barrier to wave propagation even though  $c^*$  is locally accelerated by 30% in the front of the wave packet; the reason is that at the leading edge of the wave packet no acceleration has occurred, so  $c=c(0)$ , whence  $W_g=0$  at the critical level at all times. This is some evidence of splitting of the wave packet as found by Grimshaw (1975) although this effect is slight due to the initial critical level.

The saturation limit (1.4) originally suggested by Lindzen (1981) has been imposed on this solution, and is quite crucial to the asymptotic behavior. The procedure is simply to set  $kA + kA_s \equiv \frac{1}{2}(c - \bar{u})$  whenever superadiabatic values appear (Dunkerton, 1982a; Coy, 1984). In Fig. 1 saturation first occurs near the onset of the  $A^* = .15$  contour; asymptotically the entire critical layer ( $A^* > 0$ ) is marginally stable. Because irreversibility is implicit in (1.4), a permanent mean flow change remains after the wave packet has decayed to zero. [Grimshaw (1975) recognized a permanent mean flow change in his solutions, but for an arbitrary damping not directly related to superadiabaticity.] Moreover, the permanent mean flow change includes a discontinuous "residual shock" at the lowest level of wavebreaking (Dunkerton, 1982a). This feature also appears in our numerical model, as discussed in Section 4 below.

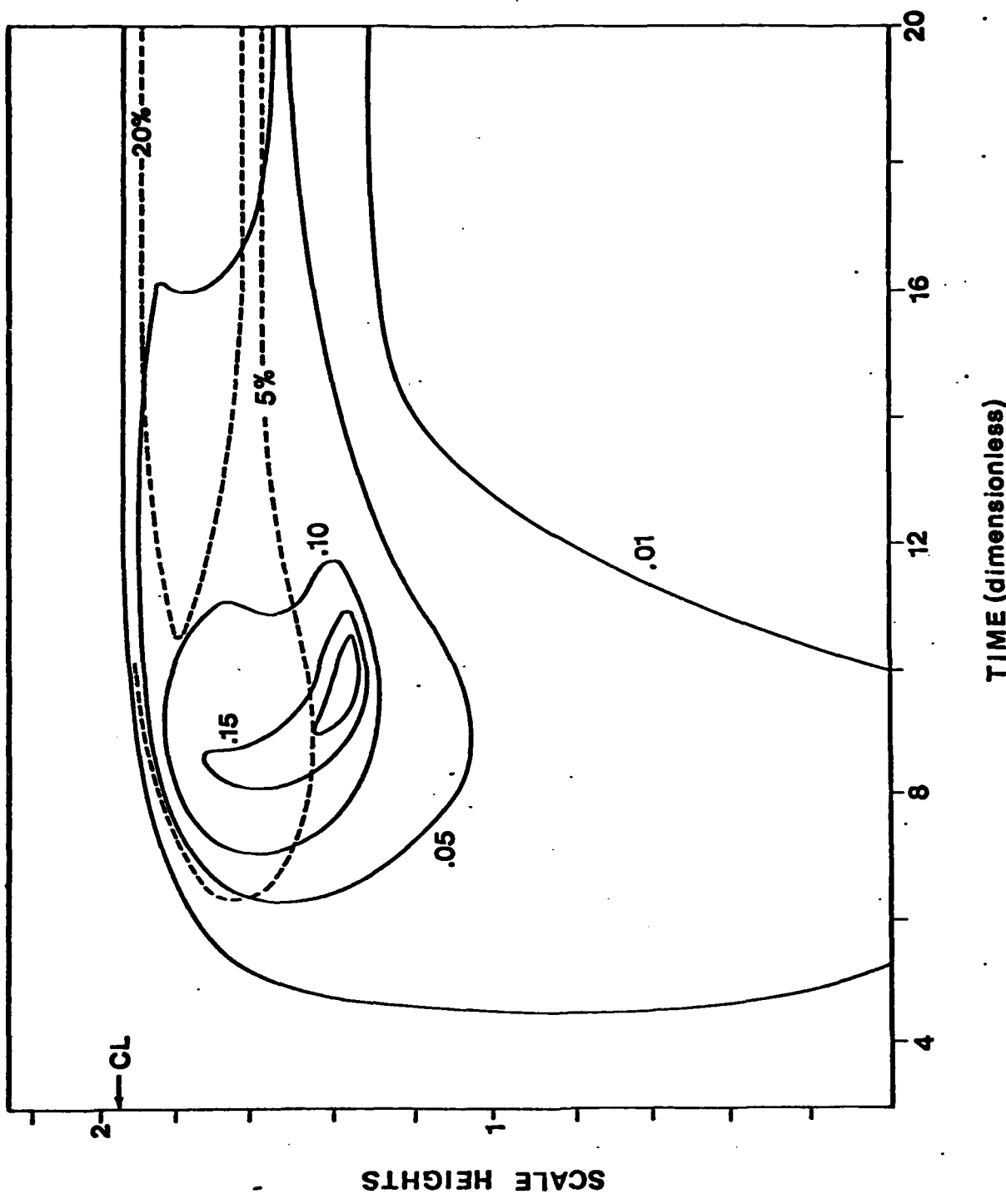


Figure 1. Semi-analytic saturated GDC solution for nondimensional wave action density and percent increase in phase speed for the case discussed in Section 2.

Without the saturation limit (1.4) or some other damping, the critical layer in this case would evolve to an unrealistic delta-function shape beneath the initial critical level. Clearly, saturation and wave absorption plays an important role in the asymptotic behavior of the critical layer.

### 3. MODEL DISCUSSION

Fritts (1979, 1982a,b) has investigated gravity wave excitation and propagation with a two-dimensional, Boussinesq, nonhydrostatic numerical model using a streamfunction-vorticity-density representation. The same numerical code is used here to study atmospheric gravity waves, but with two simple modifications: potential temperature replaces density as the conserved variable, and all nonlinear Jacobians in the wave equations are density-weighted. The vorticity and potential temperature equations for the perturbations from the zonal mean are:

$$\left( \frac{\partial}{\partial t} + \bar{u} \frac{\partial}{\partial x} \right) \eta' + w' \bar{\eta}_z - g \frac{\theta'_x}{\theta} + \exp \frac{z}{2H} \left[ J(\psi', \eta') - \bar{J}(\psi', \eta') \right] = D(\eta) \quad (3.1)$$

$$\left( \frac{\partial}{\partial t} + \bar{u} \frac{\partial}{\partial x} \right) \theta' + w' \bar{\theta}_z + \exp \frac{z}{2H} \left[ J(\psi', \theta') - \bar{J}(\psi', \theta') \right] = D(\theta) \quad (3.2)$$

where  $\psi'$  is the wave streamfunction

$$\eta' \equiv -\nabla^2 \psi' \quad (3.3)$$

and  $D(\eta)$ ,  $D(\theta)$  represent sub-grid scale diffusion and convective adjustment. (Without convective adjustment,  $D = v \nabla^2 / z^2$ , where  $v = .01 \text{ m}^2 \text{s}^{-1} \exp z/H$  and is physically almost negligible.) The primed variables are not the physical wave fields; rather

$$\begin{pmatrix} \text{physical wave} \\ \text{fields} \end{pmatrix} = \begin{pmatrix} \text{model wave} \\ \text{fields} \end{pmatrix} \times \exp \frac{z}{2H} \quad (3.4)$$

from which originates the density weighting in the Jacobian terms. (These terms are set to zero in quasi-linear simulations.) This is the only effect of compressibility on the wave fields allowed in our model. Compressibility in general will have other effects, including a contribution to the solenoidal term  $(\rho \theta)^{-1} \nabla \theta \times \nabla \rho$  and a divergence vorticity contribution  $\eta \nabla \cdot u$ . These other effects, however, are small when

$$m \gtrsim 0 \left( \frac{1}{2H} \right) \quad (3.5)$$

for the model waves, and this requirement is satisfied in the model simulations described here.

The mean flow  $\bar{u}$  represents the physical zonal mean wind, and therefore satisfies the evolution equation

$$\bar{u}_t + \frac{1}{\rho_0} (\bar{u}' \bar{w}')_z = v \bar{u}_{zz} \quad (3.6)$$

noting that  $\bar{u}' \bar{w}'$  is actually the density-weighted Reynolds stress.

Eqs. (3.1-3) and (3.5) are solved by a Fourier transform in the horizontal and finite differencing in the vertical, resulting in  $6N$  eddy equations where

$$\begin{Bmatrix} \eta'(x,z) \\ \theta'(x,z) \\ \psi'(x,z) \end{Bmatrix} = \sum_{n=-N}^N \begin{Bmatrix} \eta_n(z) \\ \theta_n(z) \\ \psi_n(z) \end{Bmatrix} \exp ikx$$

Unless specified otherwise, the basic state and wave parameters are as follows. The grid is 30 km high having 401 grid points ( $\Delta z = 75$  m). The horizontal width is 50 km and periodic boundary conditions are imposed. (This choice of grid size is well-suited to middle atmospheric gravity waves; however, the numerical code is nondimensional and can be used to study waves of any length scale.) A canonical initial mean flow is used of the form

$$\bar{u}(z) = \bar{u}(\infty) \tanh \frac{z - z_c}{D} \quad (3.8)$$

where  $\bar{u}(\infty) = 40 \text{ ms}^{-1}$ ,  $z_c = 18 \text{ km}$ , and  $D = 8 \text{ km}$ . The static stability is assumed constant in height and time:

$$N^2 g \frac{\bar{\theta}}{\theta} = \frac{\kappa g}{H} = .0003 \text{ s}^{-2} \quad (\kappa \equiv 2/7) \quad (3.9)$$

noting that  $\bar{w}' \bar{\theta}' \equiv 0$  for the Boussinesq plane wave.

The vertical boundary conditions assume a rigid upper boundary (in cases where a critical layer absorbs the incident wave) and a vertical velocity perturbation at the lower boundary representing a stationary wave:

$$w'(x, 0, t) = W(x)f(t) \quad (3.10)$$

In the experiments reported here,  $W(x)$  is a sinusoidal wave of horizontal wavelength 50 km. Three case studies are presented:

$$\text{Case I: } f(t) = \sin^2 \frac{\pi t}{t_f} \quad t < t_f \equiv 3000 \text{ s.} \quad (3.11a)$$

$$\text{Case II: } f(t) = \sin^2 \frac{\pi t}{t_f} \quad t < t_f \equiv 12000 \text{ s.} \quad (3.11b)$$

$$\text{Case III: } f(t) = \begin{cases} \frac{t}{t_f} & t \leq t_f \quad 12000 \text{ s.} \\ 1 & t > t_f \end{cases} \quad (3.11c)$$

and the forced wave amplitudes are

$$|W(x)| = \begin{cases} 3.0 \text{ ms}^{-1} & \text{(Case I)} \\ 1.5 \text{ ms}^{-1} & \text{(Case II)} \\ .75 \text{ ms}^{-1} & \text{(Case III)} \end{cases} \quad (3.12)$$

The model time step is

$$\Delta t = 12.5 \text{ s.} \quad (3.13)$$

equal to approximately 1% of the intrinsic period of the forced wave. Other details of the numerical method appear in Fritts (1979) and will not be repeated here. Discussion of the convective adjustment contribution to  $D(n)$ ,  $D(\theta)$  is deferred to Section V below.

#### 4. COMPARISON OF SEMI-ANALYTIC AND NUMERICAL SOLUTIONS

Nonlinear critical layer theory has highlighted the fact that critical levels in reality take the form of critical layers of finite thickness. However, even in linear theory the critical layer is of finite extent by virtue of the Uncertainty Principle

$$\Delta\omega\Delta T \approx 2\pi \quad (4.1)$$

The Booker-Bretherton (1967) solution unrealistically requires forcings of infinite duration  $\Delta T$  to achieve a singularity in the steady-state, i.e.  $\Delta\omega = 0$ . Under more realistic circumstances the uncertainty in wave frequency leads to a critical layer of finite thickness (Fritts, 1982b); therefore, for large-amplitude transient-impulse forcings, wavebreaking and mean flow accelerations can occur large distances above and below a supposed initial "critical level".

Case I illustrates this effect. Fig. 2 shows the mean flow in a quasi-linear simulation at  $t = 1000$  and  $12000$  s. The critical level is very poorly defined in this case. Mean flow accelerations are observed well above  $(z/z_0) = .6$ , the initial critical level of a monochromatic stationary wave. There is no evidence of the specific features of the GDC solution corresponding to this case other than the overall positive acceleration of the mean flow. Instead the mean flow behaves as if the wave packet contained a wide range of phase speeds in accordance with (4.1). This experiment and others like it suggested that the relevant value of  $\Delta T$  in (4.1) is the time duration for which  $f(t) > 1/2$ .

The shape of the evolving wave packet in  $u'$  for Case I is shown in Fig. 3 at 8000 s. The vertical wavelength decreases with time, and the wave amplitude initially increases, rapidly causing overturning in the  $\theta$ -field. The region of overturning is shown as a vertical bar to the left of each figure; note how it approximately coincides with

$$|u'| > |c - \bar{u}| \quad (4.2)$$

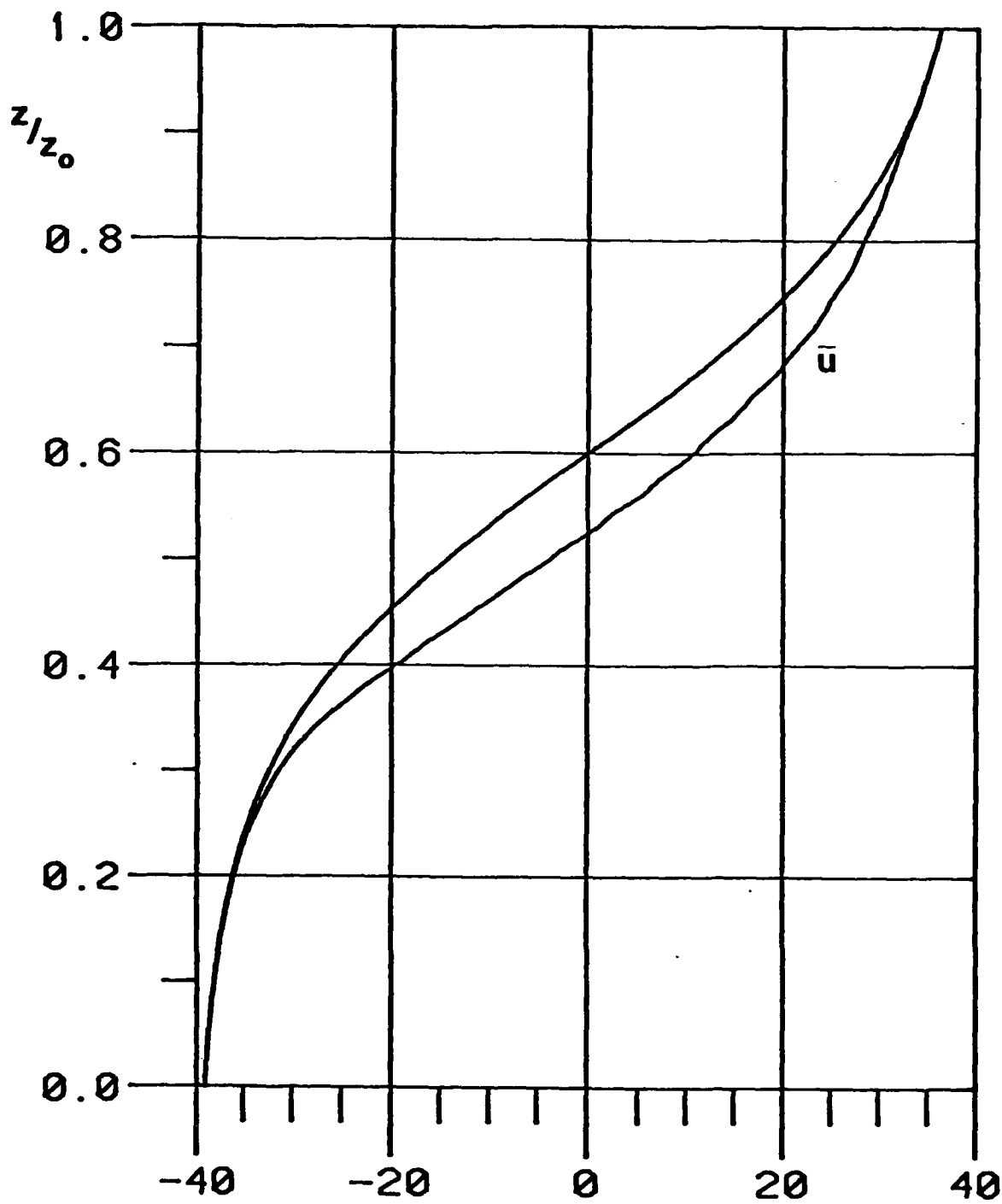


Figure 2. Zonal mean wind at  $t=0$  and  $12000$  s. for Case I. (In this and the following figures  $z_0$  is the domain height,  $30$  km.) Units:  $\text{ms}^{-1}$ .

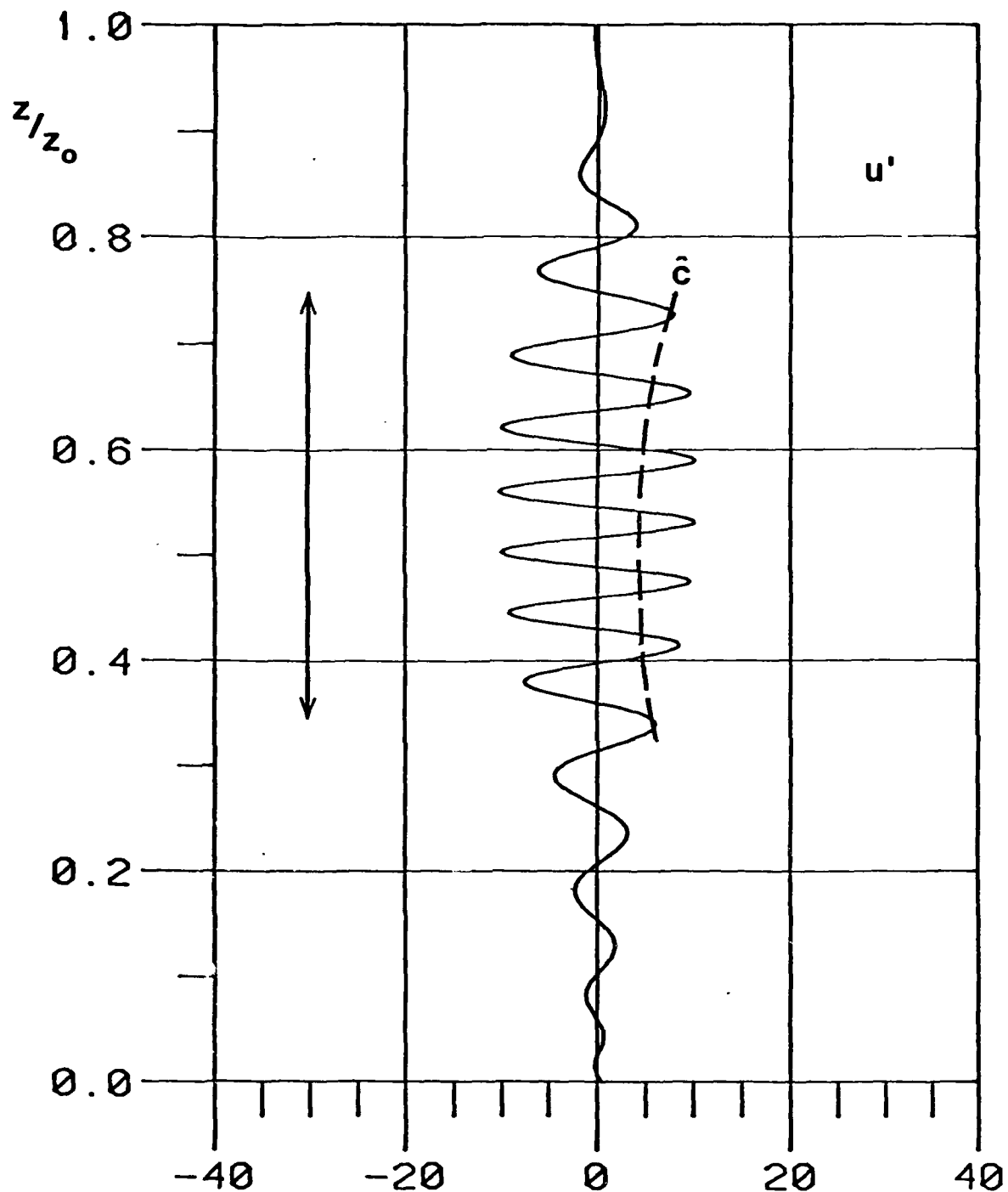


Figure 3. Perturbation zonal wind for Case I at  $t=8000$  s. Also shown are estimated intrinsic phase speed (dashed line) and region of overturning (vertical bar at left). Units:  $\text{ms}^{-1}$ .

(dashed line), where  $c - \bar{u}$  has been determined by visual inspection of the vertical wavelength in Fig. 3 and the linear dispersion relation

$$m^2 = \frac{N^2}{(c - \bar{u})^2} - k^2 \quad (4.3)$$

(Orlanski and Bryan, 1969). A kinematic explanation of (4.2) is obtained by translation to a frame of reference moving with the wave (in this case stationary); for conservative motion the  $\theta$ -surface is also a material surface along which air parcels move, therefore an overturned  $\theta$ -surface requires backward parcel motion relative to the mean flow in this reference frame. Note that the disturbance parcel motion is determined by  $u^l$ , the Lagrangian perturbation zonal velocity, which for small vertical shear is approximately the Eulerian value  $u'$  (Andrews and McIntyre, 1978; Dunkerton, 1981). Of course, although the region of overturning in Fig. 3 is quite broad compared to the GDC solution (which is qualitatively similar to that of Case II below) it is correct to speak of the overturning as a critical layer instability, keeping in mind the somewhat imprecise nature of this terminology due to (4.1). As noted in the Introduction, this critical layer effect is a specific case of wave saturation, which in general does not require an initial critical level.

The GDC solution is much more accurate when  $f(t)$  satisfies the slowly-varying approximation, i.e.

$$t_f \gg \text{forced wave period} \quad (4.4)$$

Case II illustrates a nearly "monochromatic" quasi-linear example of this type. Fig. 4 shows the mean flow evolution at  $t = 8000$  and  $12000$  s compared to its initial value (dashed line) and the saturated GDC solution (triangles). Even in this example there is still a small transmission through  $(z/z_0) = .6$  in accordance with (4.1). This is entirely a non-WKB effect as the GDC solution indicates; in the latter there is no evidence of critical level transmission. (A similar remark would seem to apply to the numerical simulation of Jones and Houghton, 1971). There is, however, no evidence of splitting of the wave packet as the GDC solution predicts.

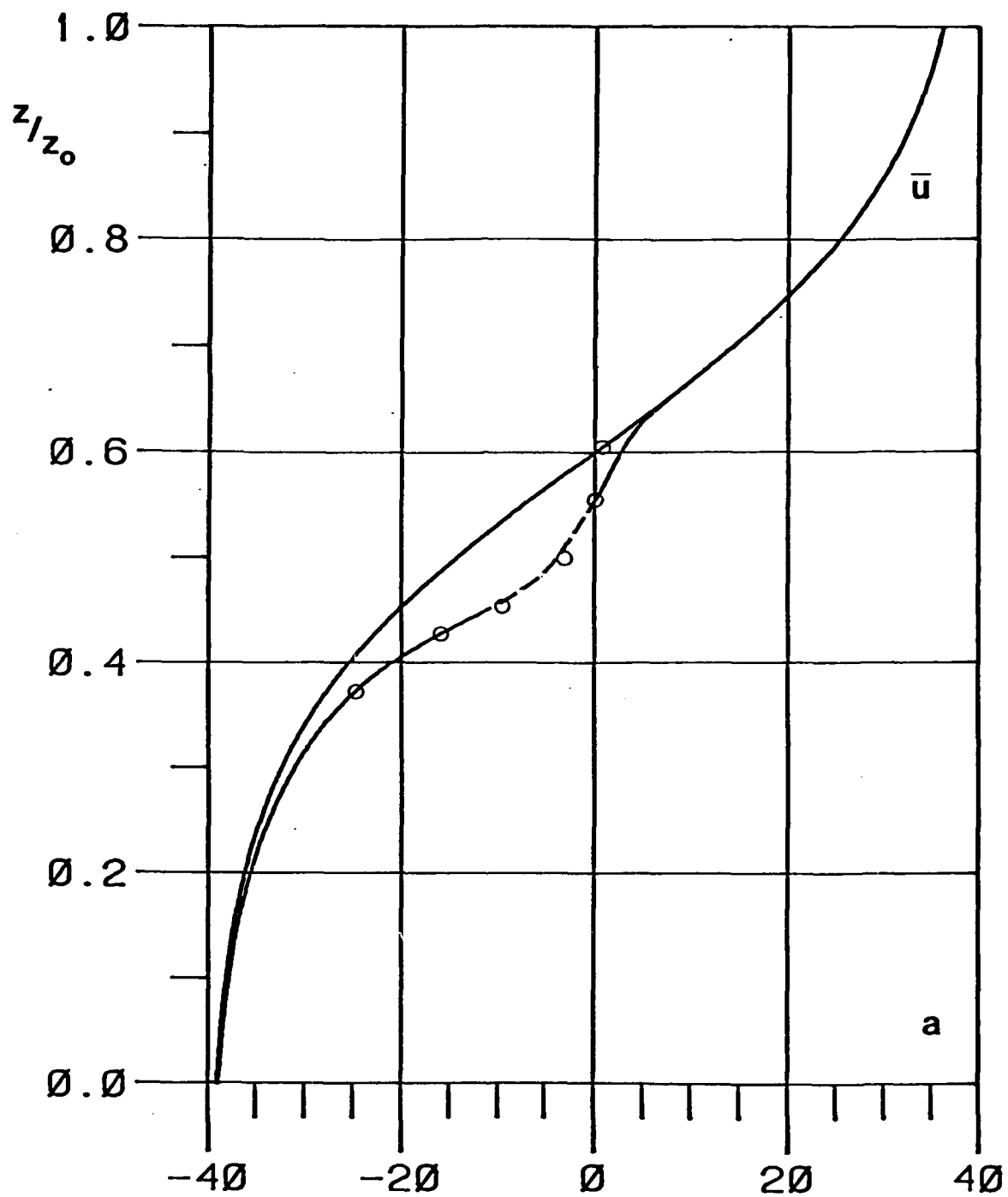


Figure 4. Zonal mean wind for Case II at (a)  $t=8000$  s, (b)  $t=12000$  s, compared to the initial mean flow and nonsaturated GDC solution. Units:  $\text{ms}^{-1}$ . (Short dashes indicate convectively unstable solution.)

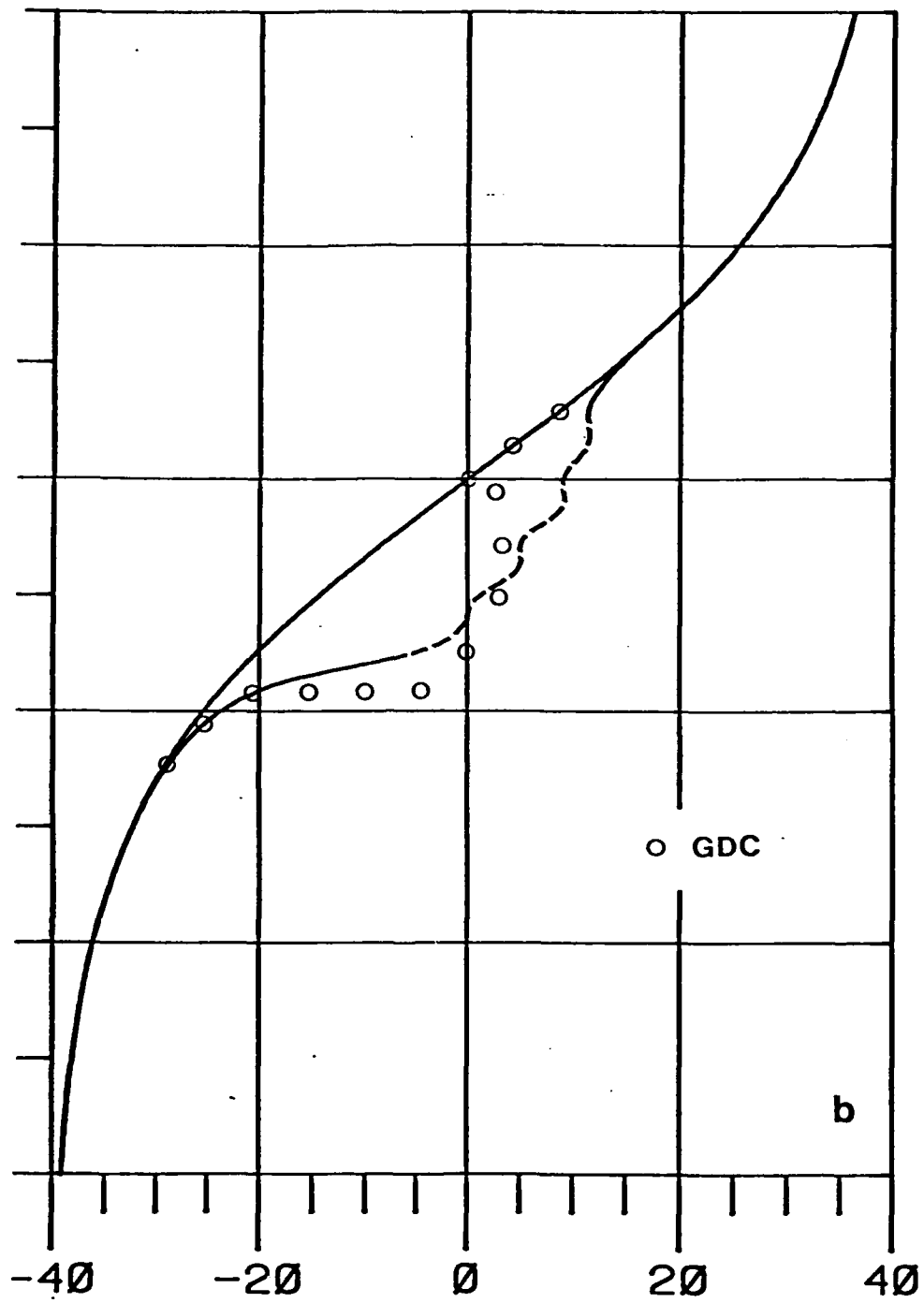


Figure 4. (continued)

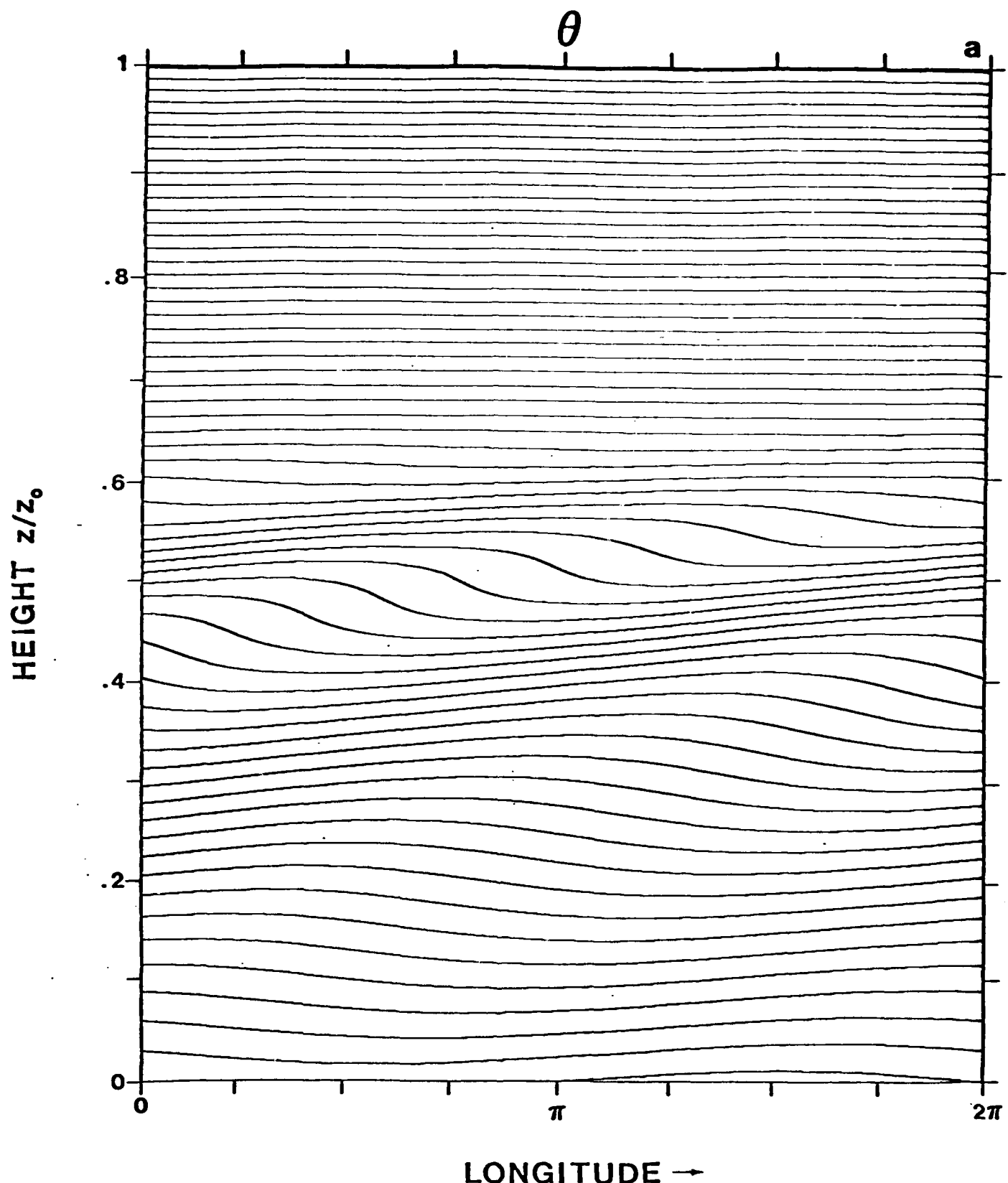
Potential temperature fields for Case II are shown in Fig. 5. The time scale for wave amplitude growth, and hence for overturning of potential temperature surfaces, is of order unity in the GDC nondimensionalization (Section 2), or about 1000 s. This is long compared to the local convection time scale

$$t_c = 2\pi \left( g \frac{\delta\theta}{\theta\delta z} \right)^{-\frac{1}{2}} \quad (4.5)$$

for the values of  $\delta\theta$  and  $\delta z$  characteristic of the overturned regions; therefore, convective breakdown is expected. But this quasi-linear model does not "see" the local regions of unstable lapse rates; as a result, the overturning continues to intensify as the vertical wavelength decreases, until the fixed-resolution model cannot resolve the vertical scale of motion any longer.

Convective adjustment, as discussed in Sections V and VI, greatly affects the critical layer behavior once the overturning begins, as might be anticipated from Fig. 5 and Eq. (4.5).

We conclude this section by noting that a highly transient forcing is not the only way to violate the slowly-varying assumptions of the GDC model. Steep mean wind shears relative to a vertical wavelength also cause a non-WKB effect. As Dunkerton (1981) noted, even the GDC solutions with their mean flow discontinuities eventually violate the WKB assumptions on which the solutions themselves depend, implying, for example, partial reflection from the internal shock. To attain downward reflection in a single wave event, wave momentum flux must be incident on the mean flow discontinuity; that is, it must be an internal, not trailing, shock. Case III illustrates a sustained forcing resulting in partial reflection. Fig. 6 displays the mean flow and eddy kinetic energy profiles for this case at  $t = 22000$  s. The steep shear zone at  $(z/z_0) = .46$  implies a mean flow  $Ri$  of 0(.8), which continues to decrease with time. A small reflected component is evident in Fig. 6b below the critical layer. This appears to be a real feature in view of the high vertical resolution employed. Some internal reflection is also evident within the (albeit unstable) critical layer. The occurrence of partial downward reflection from the critical layer seems to be a secondary effect; in



LONGITUDE →

Figure 5. Potential temperature fields  $\theta(x,z)$  for Case II at (a)  $t=6000$  s, (b)  $t=7000$  s, (c)  $t=8000$  s, and (d)  $t=9000$  s. Contour interval is .025 in nondimensional units normalized by  $\bar{\theta}(0)$ .

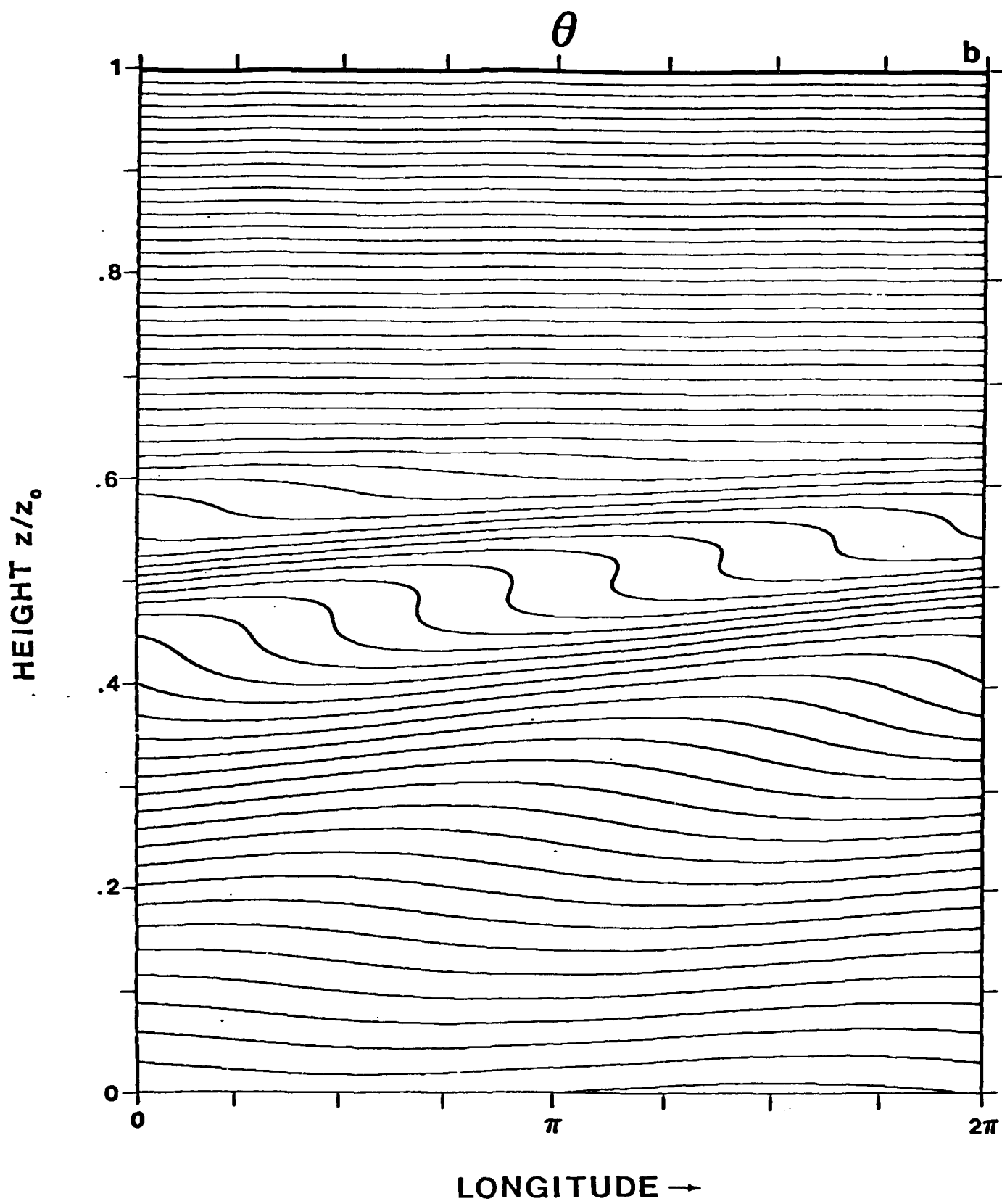


Figure 5. (continued)

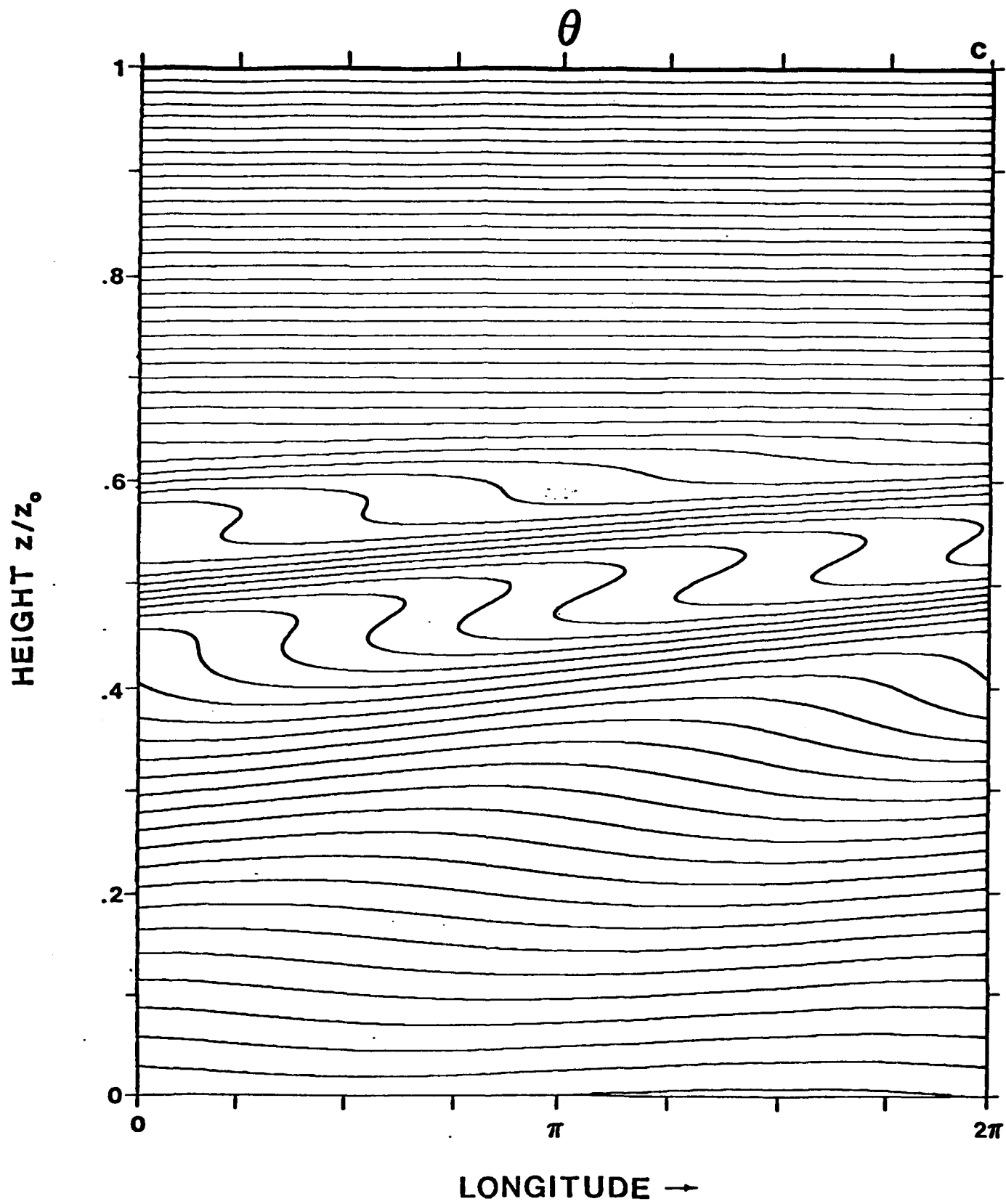


Figure 5. (continued)

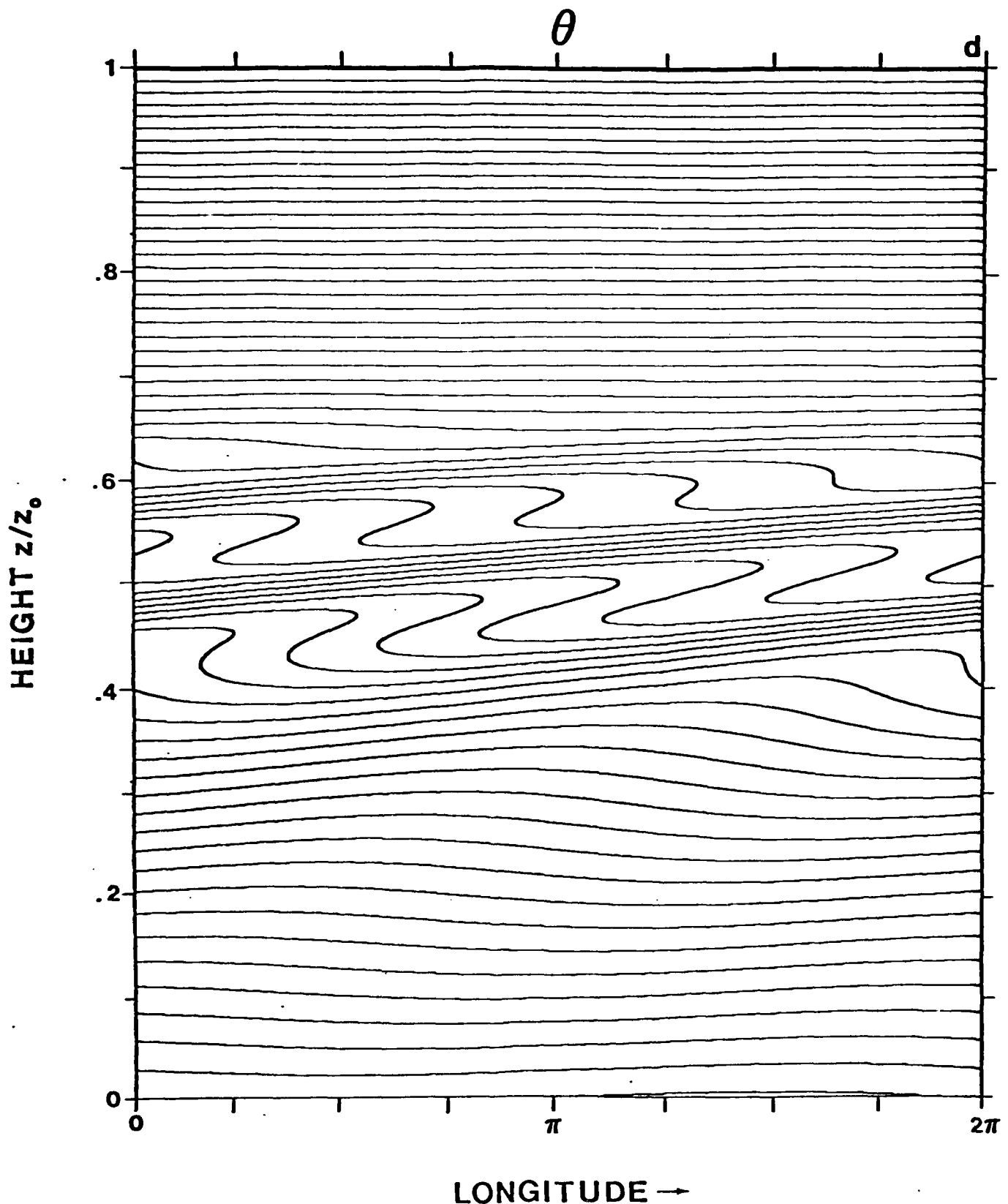


Figure 5. (continued)

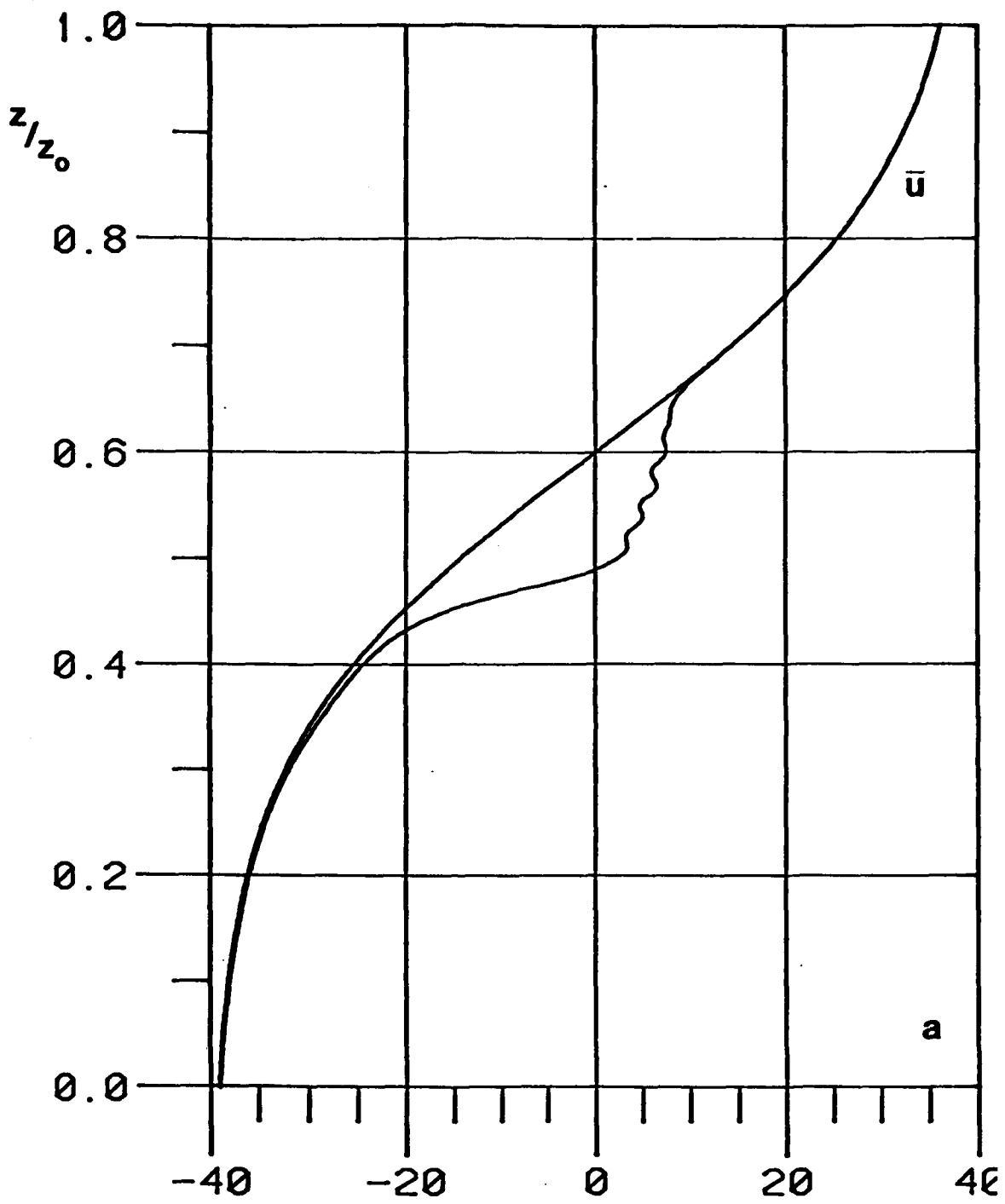


Figure 6. Partial reflection from the internal shock in Case III at  $t=22000$  s.,  
 (a) mean flow profile in  $\text{ms}^{-1}$ ; (b) eddy kinetic energy showing  
 reflected wave component below the critical layer.

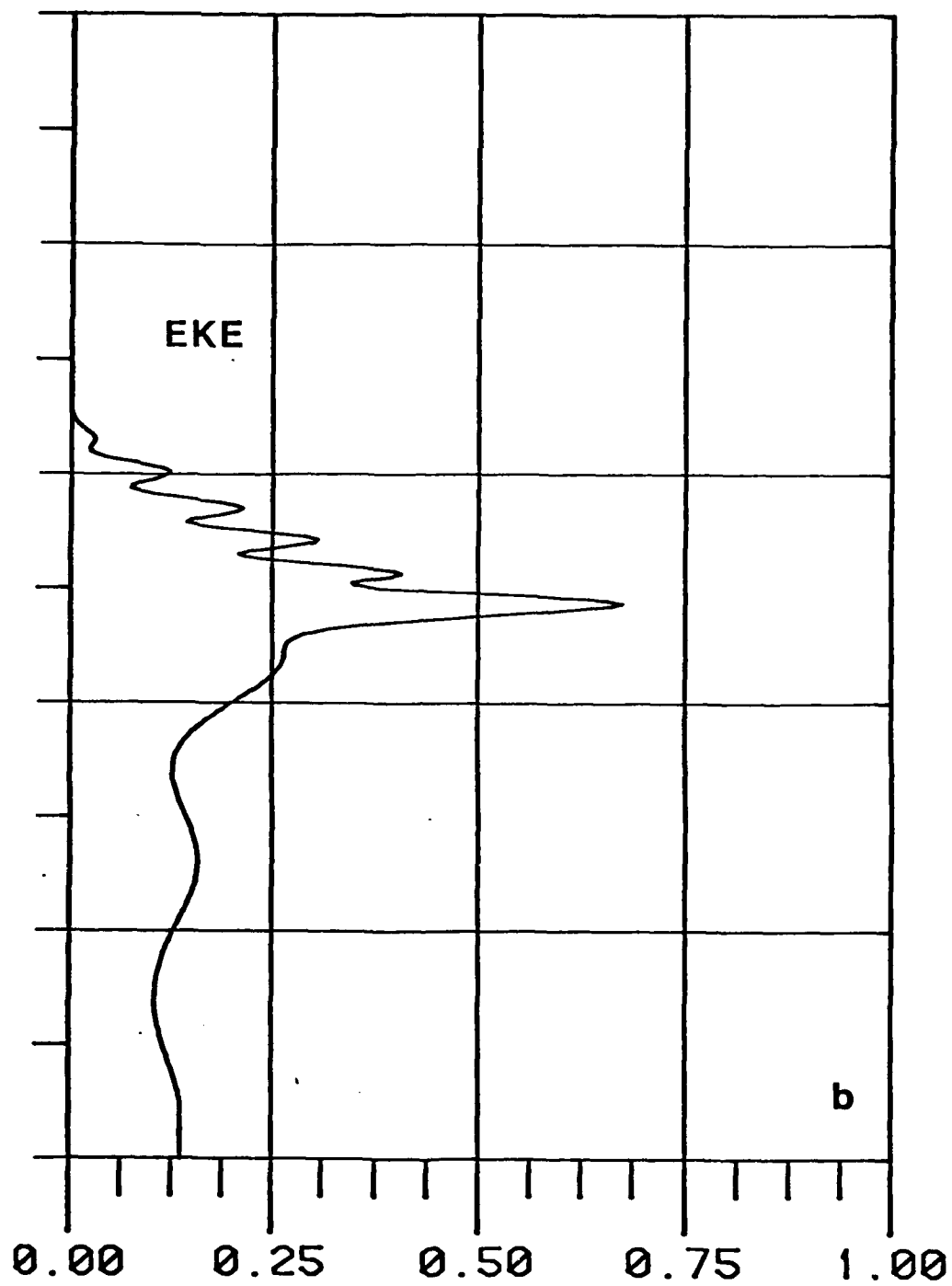


Figure 6. (continued)

this case, the internal shock is not prevented from descending on account of reflection. At  $t = 3000$  s, for example, the critical layer has descended to  $(z/z_0) = .41$ , even though the minimum  $Ri$  is still decreasing.

While in this experiment partial reflection is strictly a quasi-linear effect, nonlinear theory also predicts reflection even without taking into account the mean flow modification (Brown and Stewartson, 1980), which would in reality probably enhance the total amount of reflection (Thorpe, 1981) while possibly reducing the net mean flow modification.

Finally, note that there is some evidence of partial reflection in equatorial Kelvin waves (Salby et al, 1983). To the extent that the data is reliable, these observations might very well be the first evidence of critical layer reflection in the atmosphere. Considerably more investigation will be necessary to determine the cause of this reflection, whether it is quasi-linear or nonlinear, and associated with any well-defined critical layer.

## 5. A LOCAL CONVECTIVE ADJUSTMENT PARAMETERIZATION

The saturation limit (1.4) is a global convective adjustment parameterization, acting to restrain the forced wave amplitude independently of the wave phase

$$\Phi \equiv k(x-ct) + mz \quad (5.1)$$

Quite correctly, however, it could be objected that since unstable breakdown occurs locally within the wave where  $\theta_z < 0$ , the resulting turbulence will be phase dependent, possibly resulting in other effects besides wave absorption.

Now in principle the Boussinesq equation set (3.1-3.3) could be used, with arbitrarily high horizontal and vertical resolution, to explicitly model turbulence due to convective instability (Fritts, 1982b). However, there are certain practical and computational limits which prevent us from modelling the fluid motions at ever-smaller scales, towards which convective instabilities will inevitably cascade. Therefore a turbulence parameterization of the sub-grid scale motion is required.

Towards this end we have developed and successfully implemented a convective adjustment scheme which is built on the simple premise that convective instability acts to eliminate superadiabatic lapse rates. A novel feature of our scheme is the avoidance of any reference to "eddy diffusion". Instead it is assumed, appropriate to all the specific examples we are currently studying, that convective instabilities are rapid, steady, and efficient in their "neutralization" of unstable flow profiles. This assumption is identical to that underlying the saturation limit (1.4) and its use in the GDC model. The essential difference, however, is that convective adjustment is now applied locally within the wave.

The purpose of this and the following section is to describe the adjustment procedure and to show how it dramatically affects the critical layer evolution in the case studies cited earlier. These examples are quite idealized and of limited interest; nevertheless, the convective adjustment parameterization has been successfully implemented in very complex flow profiles with 64-harmonic resolution, and later reports will present some

examples of its use in more complex and realistic wave, mean-flow interaction problems.

a. Earlier turbulent adjustment schemes

Previous authors have attempted to account for dynamical or convective breakdown in unstable gravity wave motion (e.g. Orlanski and Ross, 1973; Klemp and Lilly, 1978; Peltier and Clark, 1979; Fua et al, 1982; Durran and Klemp, 1982). These suggested turbulence closure schemes have little in common except to enhance the turbulent eddy diffusion within "dynamically unstable" ( $Ri < 1/4$ ) or convectively unstable ( $Ri < 0$ ) regions.<sup>1</sup> An exception is the isentropic coordinate model of Klemp and Lilly (1978) in which an instantaneous turbulent adjustment procedure was applied when  $Ri < 1/4$ .

It is beyond the scope of this paper to review each scheme in any detail. However, it is worthwhile to note that in each case the adjustment is local; e.g. local turbulent diffusion is of the form

$$D = \nabla \cdot v(x) \nabla \quad (5.2)$$

In a longitudinally-dependent flow,  $v(x)$  acts to scatter wave energy among all Fourier harmonics, in a manner analogous to that of the advectively nonlinear Jacobians, which (5.2) is intended to parameterize at sub-grid scales. Following Fua et al (1982), this scattering process will be identified as wave-turbulence interaction.

b. Convective adjustment

For several years, convective adjustment has been employed in general circulation models to neutralize convectively unstable lapse rates due to radiative heating in the lower troposphere. Climate modellers working at long time scales seek to avoid both explicit calculation and diffusive parameterization of convection effects. Instead, the quite reasonable assumption is made that convection quickly acts to eliminate superadiabatic regions.

In adopting this approach, which actually bears a slight resemblance to that of Klemp & Lilly (1978), we regard the gravity wave critical layer breakdown as a problem eminently suited to convective adjustment, provided

<sup>1</sup>The quote marks indicate our understanding that  $Ri < 1/4$  is not a general dynamical instability criterion for gravity waves.

that certain simple criteria are satisfied. First, the Reynolds and Rayleigh numbers must be adequately large such that diffusion plays no role at the resolved scales of motion. In the calculations presented here  $v = .01 \text{ m}^2 \text{s}^{-1}$  and is practically negligible at the model scales. Second, the overturning must occur slowly relative to the rate of growth of convective instabilities (4.5) -- a criterion with which surfers are personally familiar.<sup>2</sup> This condition is, of course, quite easily satisfied in inviscid gravity-wave critical layer evolution and for the long horizontal scales employed here.

Convective adjustment, when appropriate, has at least three important advantages over enhanced turbulent diffusion. First, it efficiently replaces large eddy diffusivities and their large gradients which might be required to maintain near-neutral lapse rates. Second, the effect of convective adjustment immediately extends outside the unstable region, unlike all turbulent diffusion schemes written in the form  $v(Ri)$  or  $v(Ra)$  which incorrectly (or at best, inefficiently) identify regions affected by instabilities as satisfying some local instability criterion. Third, a convective instability parameterization applied in a nonlinear code allows the model itself to determine whether a gravity wave is dynamically unstable, including K-H modes of instability.

Initially it was thought that convective adjustment would be unsuitable in a dynamical model, possibly acting to "shock" the numerical wave fields. In general, however, this problem was not at all severe. Nevertheless, to eliminate any potential problems of this sort, it was found that partial convective adjustment was virtually as efficient as a total adjustment in maintaining near-neutral lapse rates within the wave. This procedure also allows a convection time scale to re-enter the problem when desired.

<sup>2</sup>The breaking surface wave manifests large horizontal parcel accelerations relative to gravity (Baker et al, 1982) and therefore the heavier fluid can temporarily find itself suspended over the lighter fluid. The pail of water swung in pendulum fashion over one's head is (hopefully) convectively stable also; in (4.5) it is the gradient parallel to the net acceleration which is relevant (Drazin and Reid, 1981).

### c. Relaxation to neutral equilibrium

The convective adjustment procedure begins with an FFT to physical space to examine where (1.5) is satisfied. An adjusted  $\theta^E(z)$  column is then returned to the main program as shown in Fig. 7. This procedure is repeated for each column until a convectively stable  $\theta^E(x,z)$  field is created. The new field  $\theta^E$  is regarded as an equilibrium field which has conserved total potential temperature (cf. Fig. 7).

Following the vorticity diffusion approach of Orlanski and Ross (1973), an equilibrium vorticity profile  $\eta^E(z)$  is also calculated, column by column, mixing together the values of  $\eta$  at each vertical group of grid points affected by the  $\theta$ -adjustment in Fig. 7. In such regions  $\eta^E(z)$  is set equal to the average of  $\eta$  over these points. Other, more complicated  $\eta^E$  profiles were constructed similarly (by weighting the average relative to the distance from the endpoints, for example) but with little observed effect. This procedure is analogous to the vorticity diffusion used by Orlanski and Ross (1973). Convection will of course create vorticity locally, but the integrated effect between any two stable isentropes is zero by Kelvin's circulation theorem. Like Orlanski and Ross, we assume that whatever sub-grid scale structure is created in the vorticity field is not relevant to the larger-scale dynamics. Incidentally, since to within the approximations of the model, density is nearly constant over a vertical wavelength, no attempt has been made to conserve the mass-weighted variables  $\rho_0 \theta$ ,  $\rho_0 \eta$  although in general this should be done.

Finally, the new vorticity and potential temperature fields are determined by the frictional relaxation formulas

$$\theta_{\text{new}} = (\omega t)^E + (1 - \omega t)\theta_{\text{old}} \quad (5.3a)$$

$$\eta_{\text{new}} = (\omega t)^E + (1 - \omega t)\eta_{\text{old}} \quad (5.3b)$$

The inverse convection time scale  $\omega$  could be regarded as the single floating parameter in this "closure" scheme. Although in general  $\omega$  could be calculated explicitly as

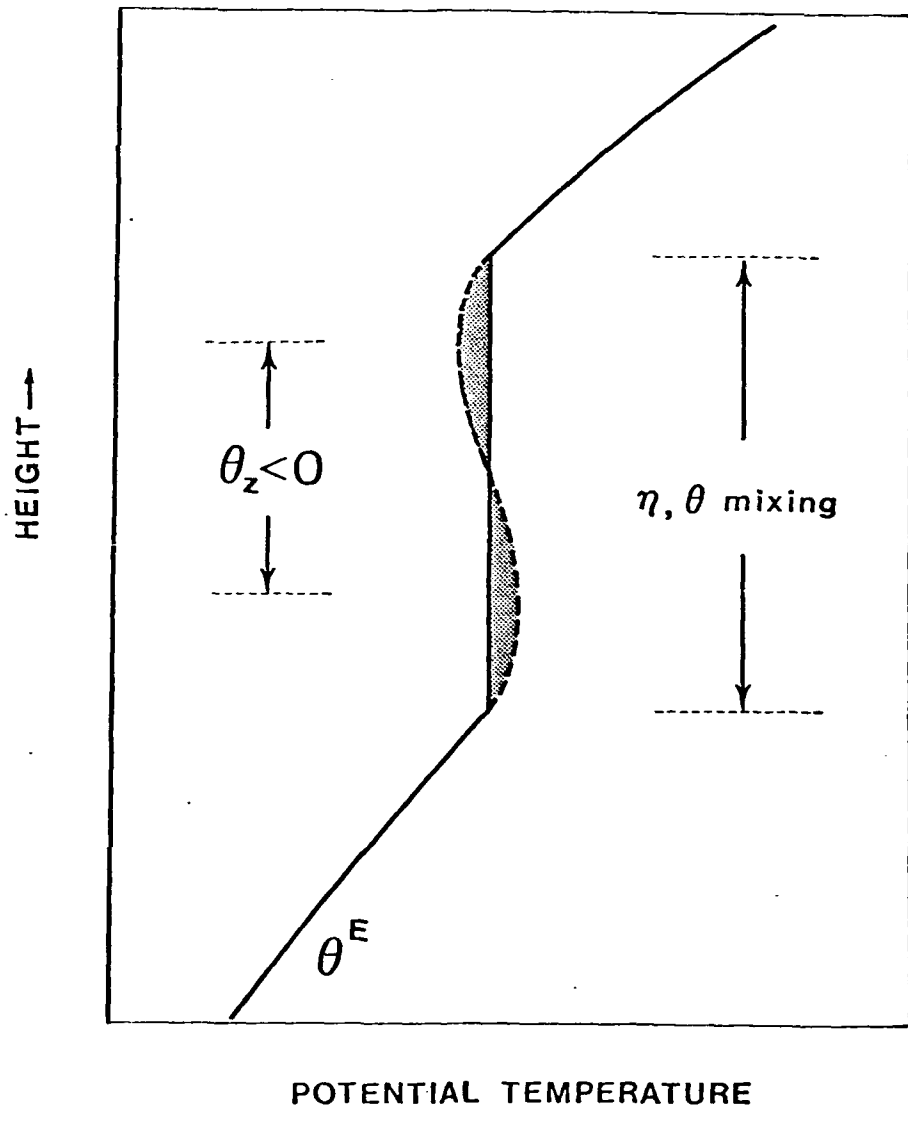


Figure 7. Illustration of how a unique equilibrium potential temperature profile  $\theta^E(z)$  is created from an unstable  $\theta$ -column. The shaded regions represent equal mass (mass-weighted in general) thus conserving potential temperature. The equilibrium vorticity profile  $\eta^E(z)$  is set equal to the average value of  $\eta$  in the mixed region; outside this region,  $\theta^E \equiv \theta$  and  $\eta^E \equiv \eta$ .

$$\alpha = 0(t_c^{-1}) \quad (5.4)$$

for our observed values of  $t_c$  it seemed desirable to instead work with a fixed value, e.g.

$$\alpha\Delta t = 0.125 \quad (5.5)$$

because calculated values of  $\alpha\Delta t$  would be near unity, possibly causing spurious numerical effects. Interestingly, the partial relaxation (5.5) seems able to stabilize the flow in the examples discussed here, without causing numerical side effects.

## 6. IRREVERSIBLE ABSORPTION AND MEAN FLOW ACCELERATION AT THE CRITICAL LAYER

Both the transient-impulse (Case I) and nearly monochromatic forcing (Case II) provide excellent case studies for convective adjustment. Because Case II compares especially well to the GDC solution, it is of interest to first compare the "saturated" numerical and semi-analytic solutions for this case.

Fig. 8 displays the potential temperature fields for the quasi-linear Case II with partial convective adjustment according to (5.3) and (5.5). Note that in Fig. 5d the convection time scale is  $O(110$  s.) so that (5.5) actually represents a somewhat slower time scale of  $O(250$  s.) which, nevertheless, virtually eliminates the superadiabatic regions. Small regions of overturning in Fig. 8d are probably the result of the horizontal truncation used in this case ( $N=8$ ). A companion experiment with  $\alpha\Delta t=1$ , but with the adjustment applied once every 8 time steps, yielded very similar results but including a significant, and possibly spurious, wave 1 component reflected from the critical layer.

Fig. 8d ( $t=12000$  s.) is characteristic of the asymptotic state, including an undisturbed flow at low levels, a turbulent critical layer bounded underneath by a steep gradient in wave amplitude and mean flow, and an almost undisturbed flow above the critical layer. Curiously, comparison of the "saturated" and unstable solutions suggested that convective adjustment acts to slightly reduce the amount of transmitted wave energy in this case, which is in both cases associated with the transient switch-on of the forced wave.

What is of most interest in Fig. 8d is the reduction in wave amplitude clearly evident in the weakening of the "braids", or dense-contour regions, which up to this point have been intensifying and would otherwise continue to do so in the absence of convective adjustment. Fig. 9 confirms that the domain-integrated eddy kinetic energy is at this time down by a factor of 3 from the unstable case. Wave action conservation implies a reduction in wave energy in both cases as the critical level is approached, but the critical

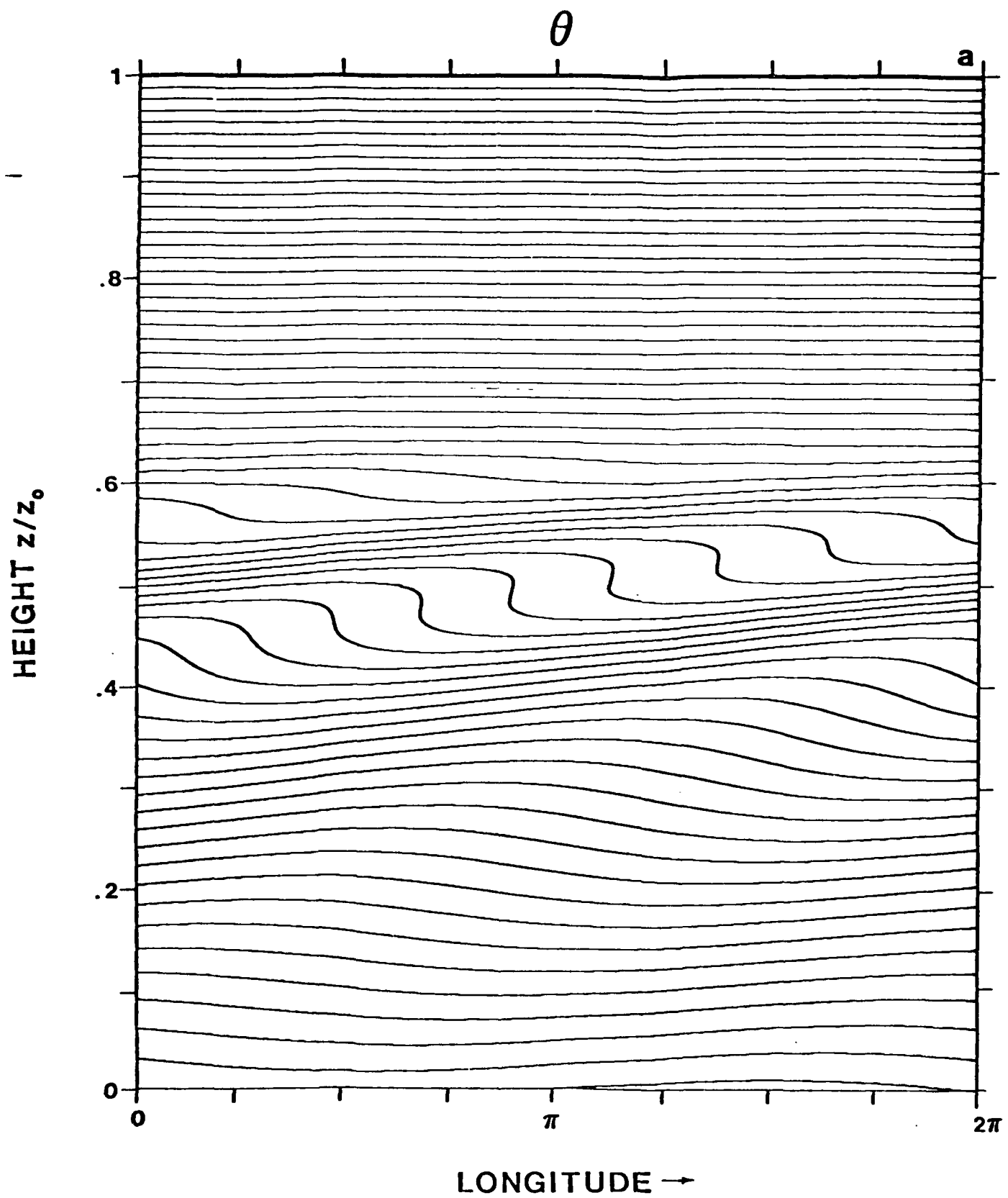


Figure 8. Potential temperature fields  $\theta(x, z)$  for Case II with convective adjustment; (a)  $t=7000$  s., (b)  $t=8000$  s., (c)  $t=9000$  s., (d)  $t=12000$  s.

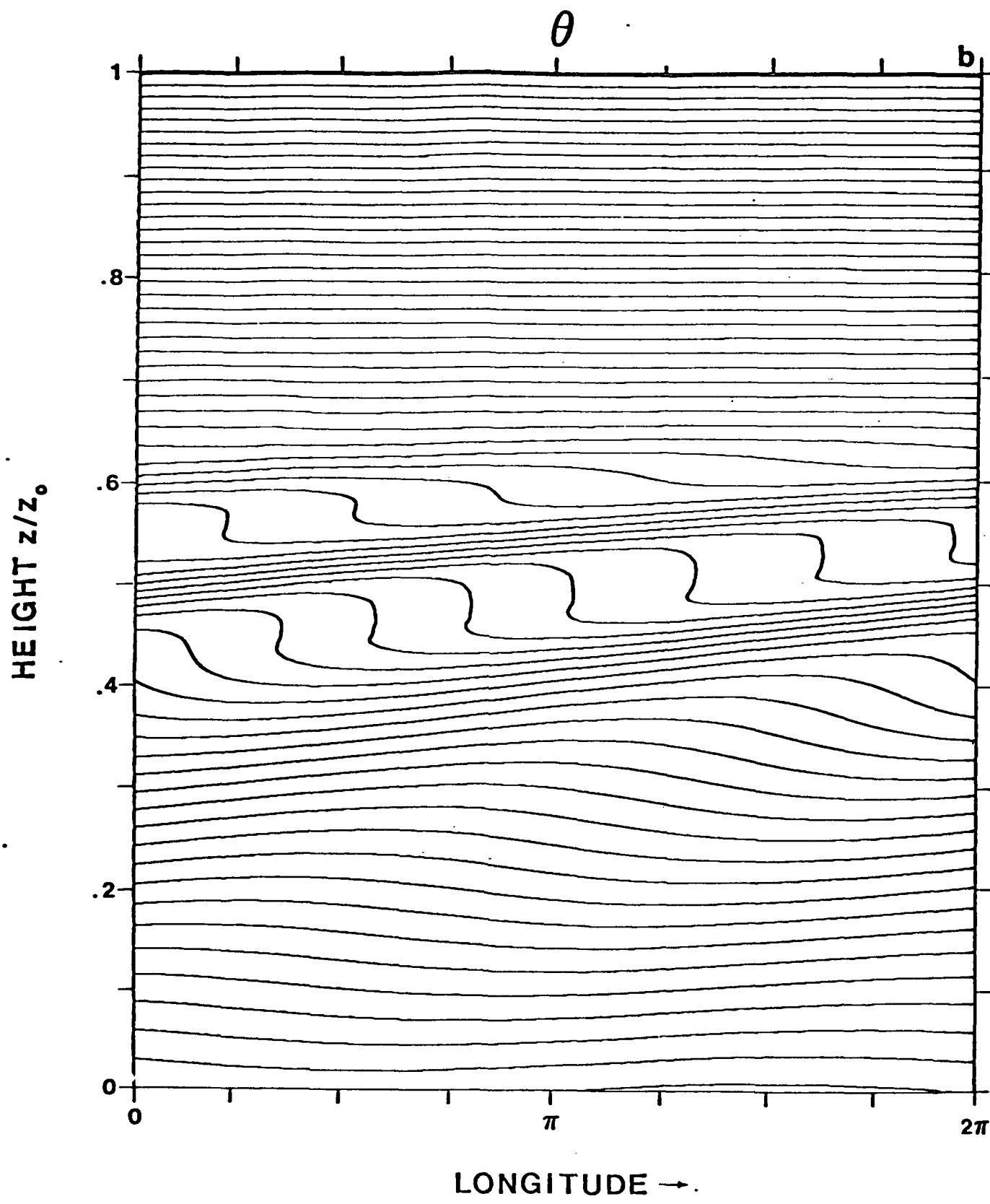


Figure 8. (continued)

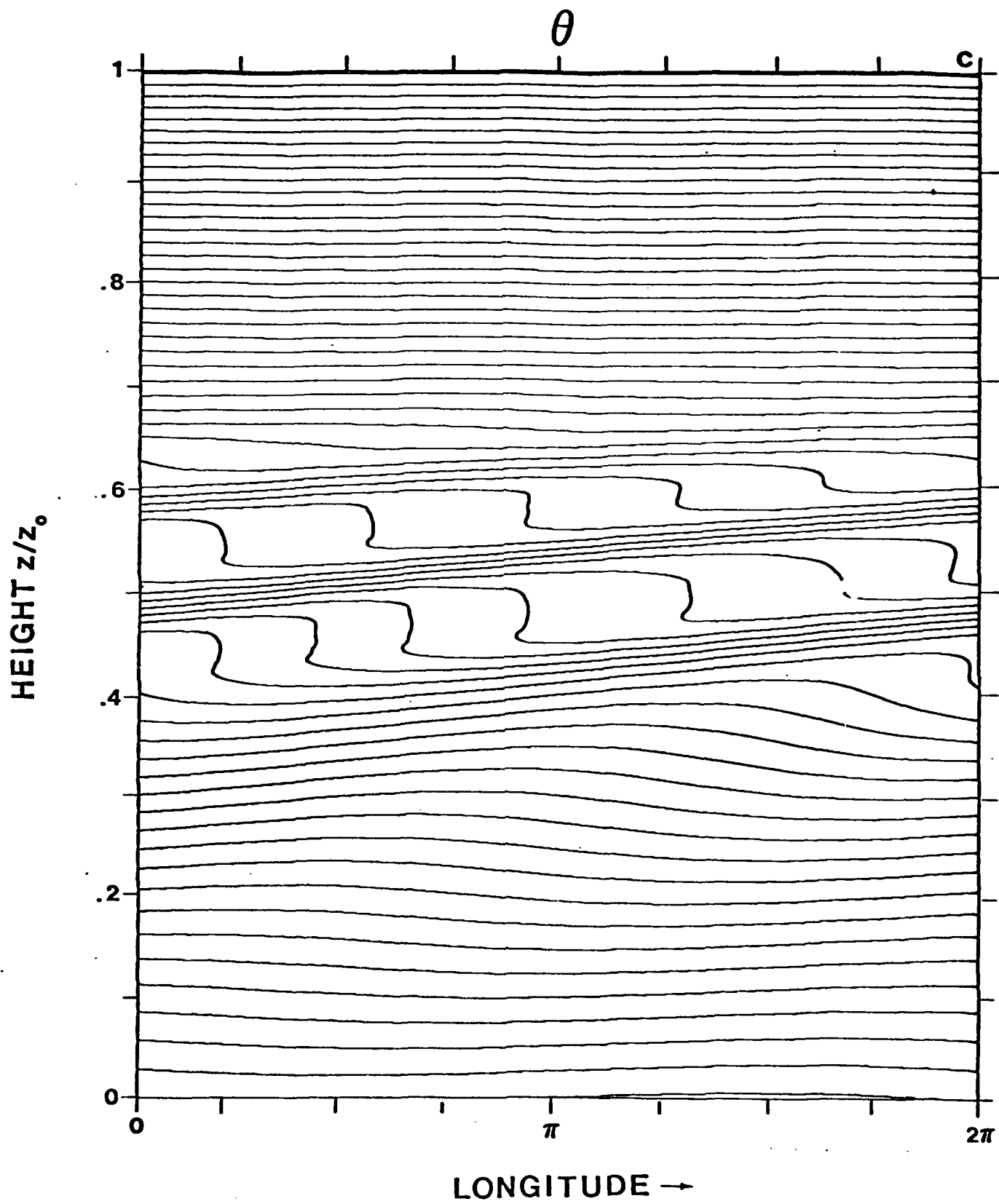


Figure 8. (continued)

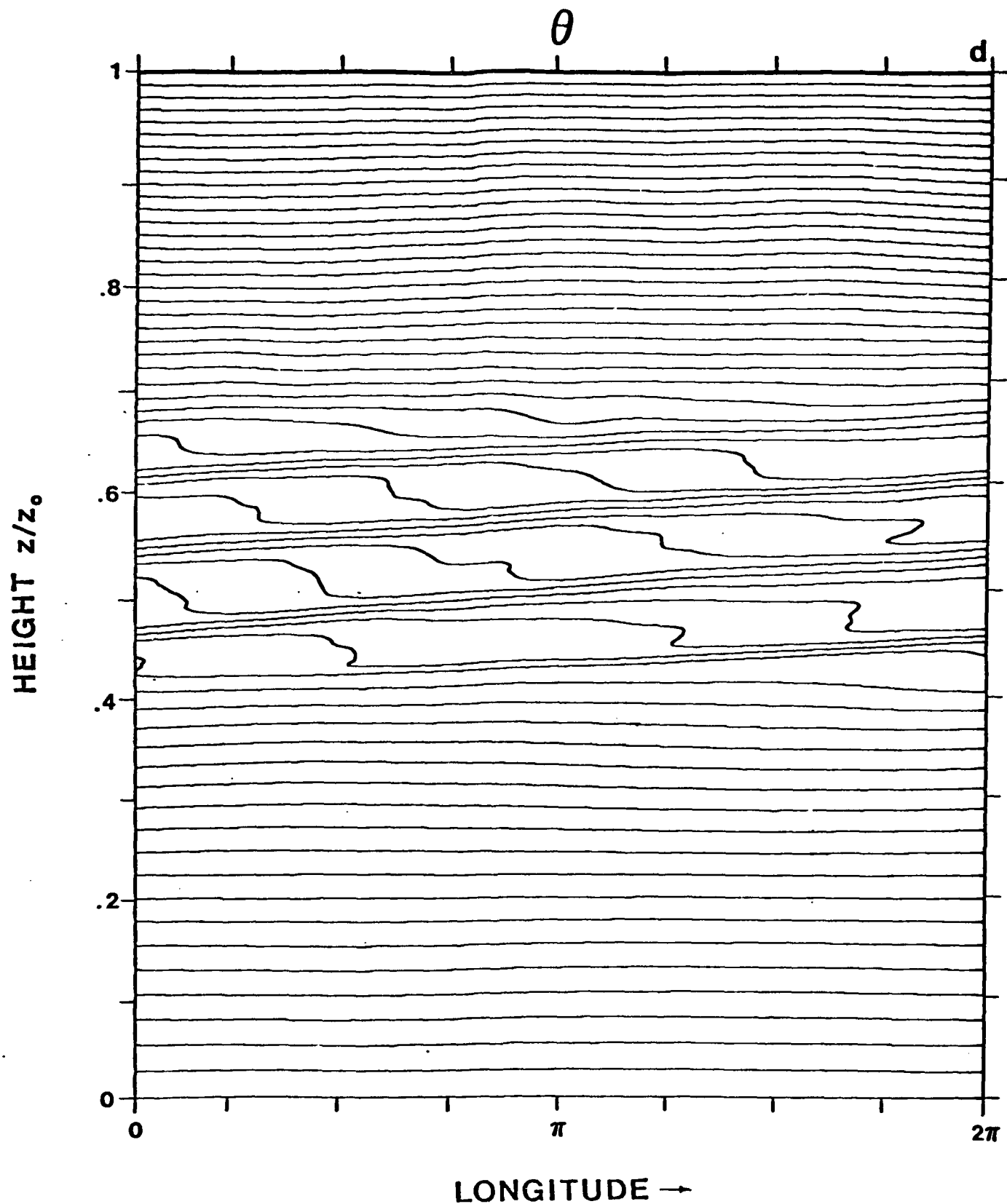


Figure 8. (continued)

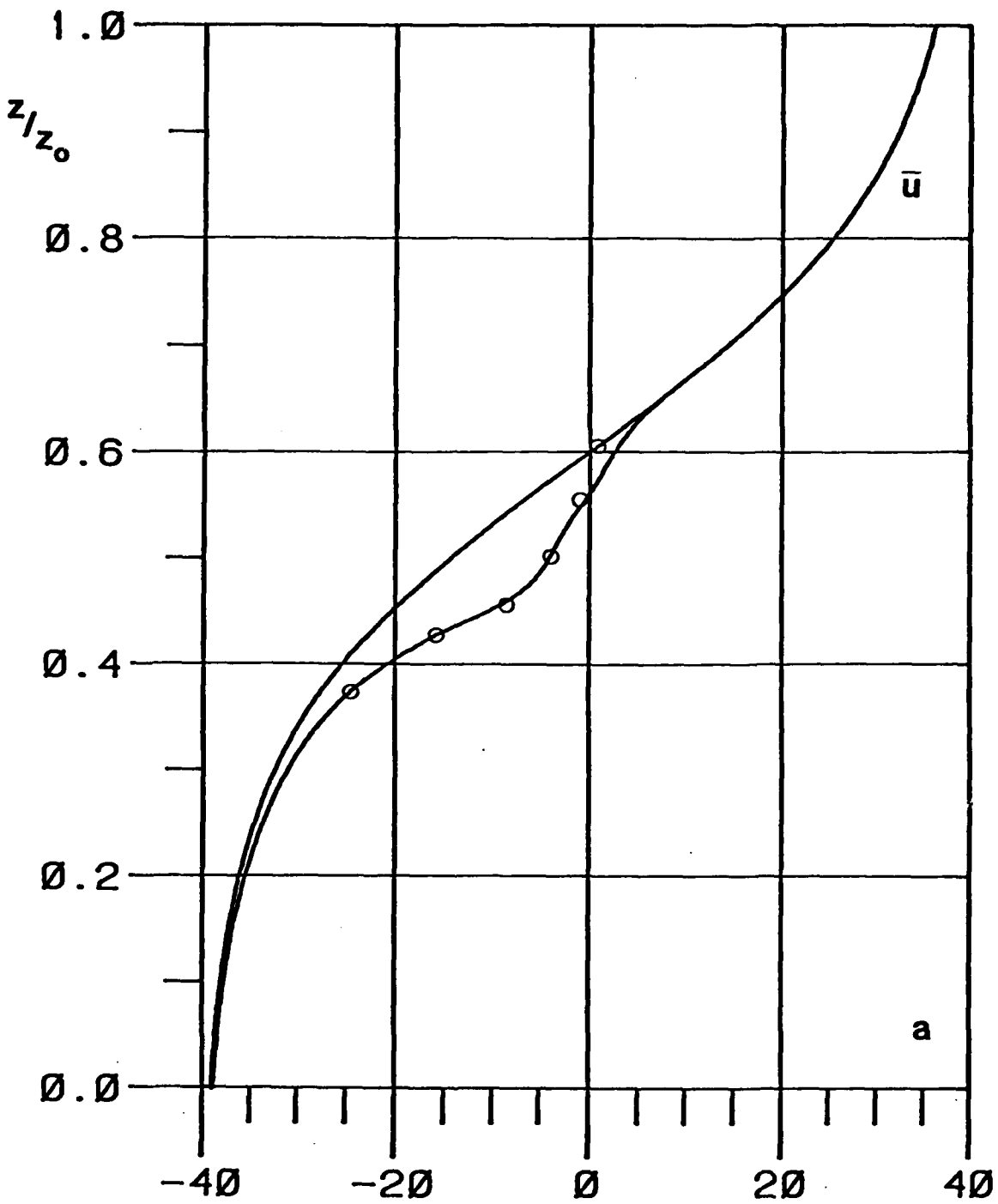


Figure 9. Zonal mean wind at (a) 8000 s., and (b)  $t=12000$  s. for Case II with convective adjustment, compared to the initial mean flow and saturated GDC solution. Units:  $\text{ms}^{-1}$ . (Short dashes indicate marginally stable solution.)

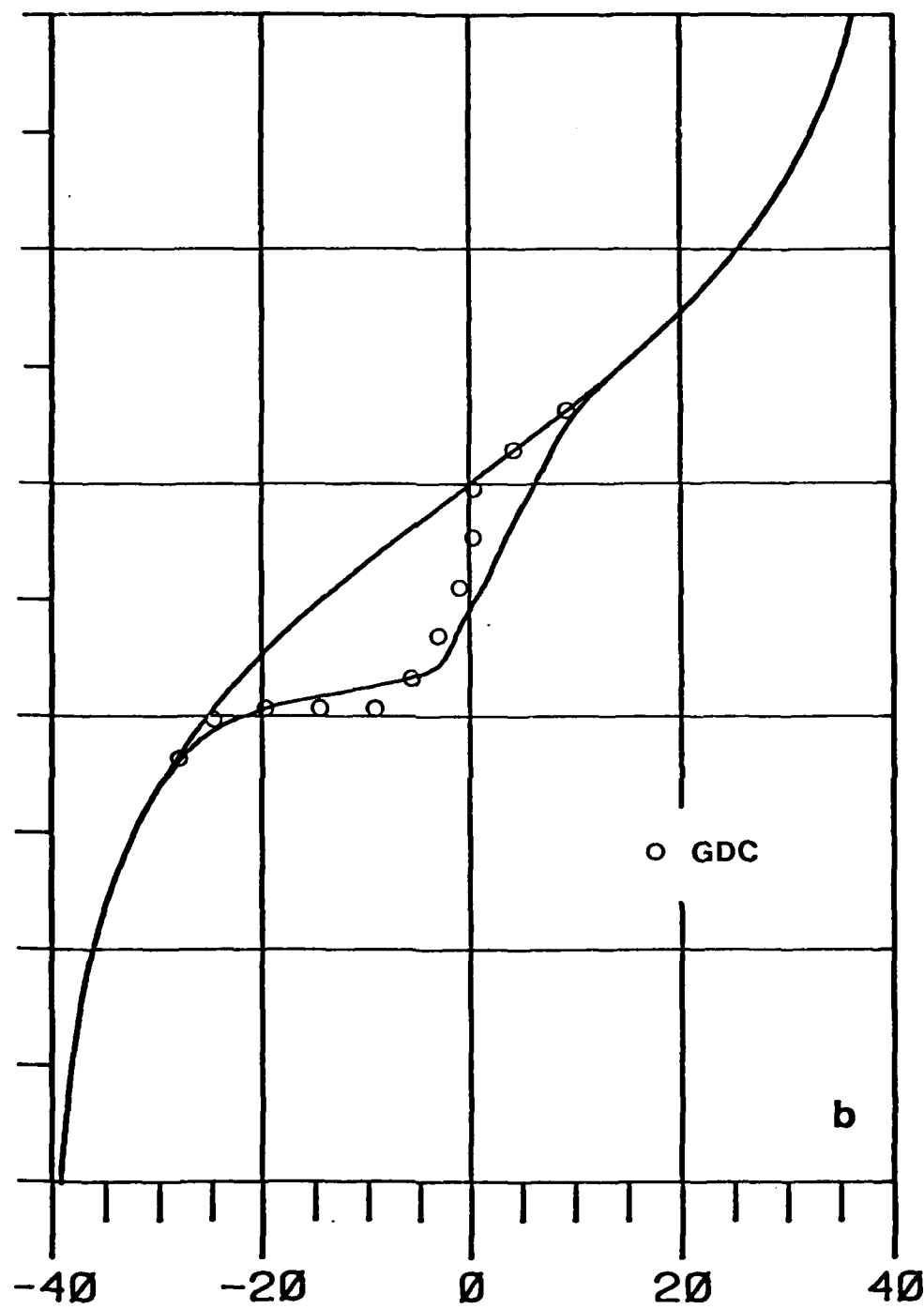


Figure 9. (continued)

layer absorption is now dramatically enhanced due to convective adjustment. Most of the wave energy has gone to the mean flow; in Fig. 9 only a small fraction has been transferred via parameterized wave-turbulence interactions to the higher harmonics. It is likely that more energy would have found its way to the higher harmonics had the wave-wave interactions been included; however, for near-stationary waves all but waves 1 - 3 are evanescent away from the critical layer in this mean wind profile when the horizontal scale is 50 km.

Inasmuch as the results of this particular case seem to confirm Lindzen's (1981) global amplitude balance model, it is not surprising that the mean flow evolution to a large extent also proceeds in accordance with the saturated GDC solution. Fig. 10 indicates that the discontinuity in mean flow coincides with the residual shock of the GDC solution at  $(z/z_0) = .41$ . To suppress small scale noise in  $\bar{u}$ , a 1-2-1 smoother has been applied to the mean momentum correction  $\rho_0(\bar{u}-\bar{u}_0)$ , equivalent to an enhanced global eddy diffusion of  $0(44 \text{ m}^2 \text{s}^{-1})$ .

Comparison of Fig. 10 with Fig. 4b shows larger (smaller) accelerations at the bottom (top) of the critical layer in Fig. 10, consistent with theory (Dunkerton, 1982a). There is a qualitatively similar mean flow change in both cases, but the fact must not be overlooked that in Fig. 10 this change approximately represents the asymptotic effect, whereas Fig. 4b does not since no dissipation has occurred there. A permanent change in  $\bar{u}$  has now occurred, over a finite height interval, due to convective adjustment.

Continuing the numerical simulation to  $t=20000$  s. did not reveal any change in the thickness of the critical layer in agreement with the semi-analytic theory, and asymptotically the entire critical layer seemed to remain marginally unstable.

Case I, the transient-impulse experiment, was also repeated with convective adjustment applied, and with similar results (not shown). In this case overturning occurs more rapidly due to the larger wave amplitude; however, convective adjustment once again eliminated the superadiabatic regions. There is considerable transmission through the initial critical level in this

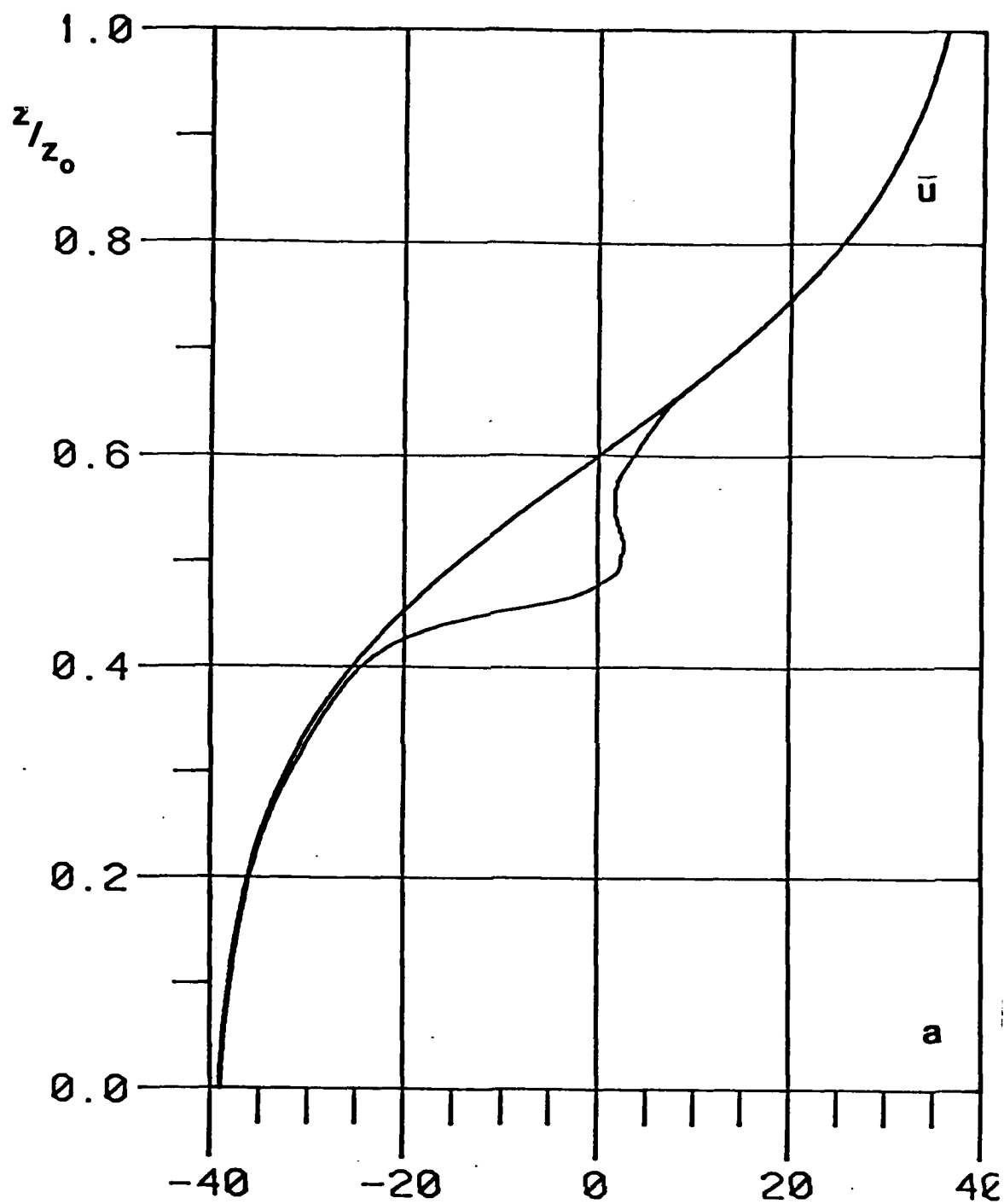


Figure 10. Results for Case III, as in Fig. 6, but with convective adjustment.

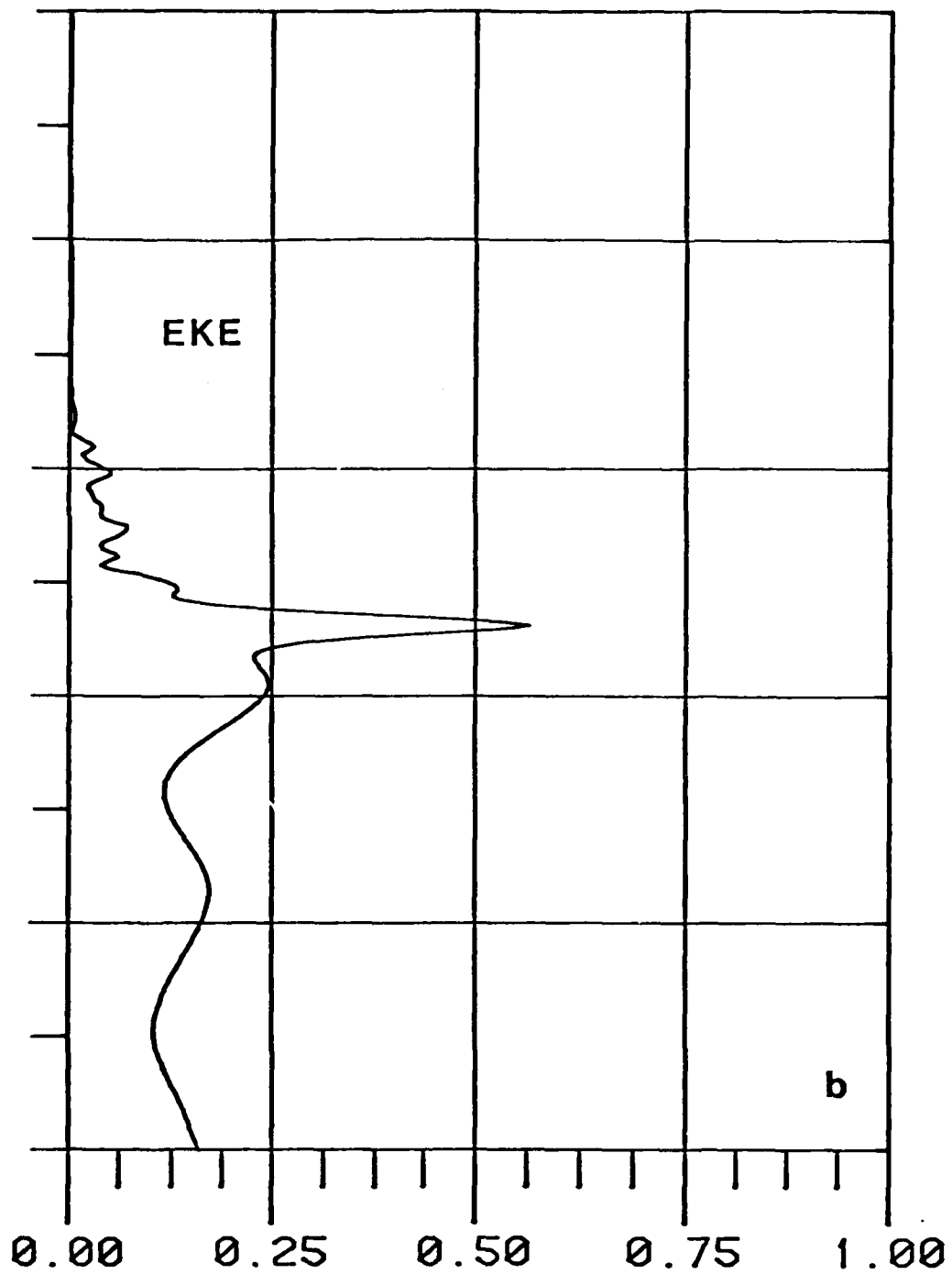


Figure 10. (continued)

case, but this is entirely the effect of the impulsive forcing, not convective adjustment. However, in this case convective adjustment did effect a permanent mean flow change well above the initial critical level due to the over turning observed there (cf. Figs. 2 and 3). The magnitude of this mean flow modification above the initial critical level was found to be slightly reduced by convective adjustment, as we would expect, but the vertical extent of the transmitted component remained about the same.

The effect of convective adjustment on Case III, the experiment with sustained forcing, is shown in Fig. 10. Saturation has increased the strength of the internal mean flow shock, resulting in a slightly larger reflected component, and has severely reduced the reflection within the unstable critical layer. Fig. 10a provides perhaps the best comparison to Coy's (1984) monochromatic slowly-varying results, with the formation of a secondary mean flow maximum beneath the initial critical level.

## 7. CONCLUSION

The author's research has attempted to test the accuracy of the semi-analytic GDC method along two lines; first, with regard to the accuracy of the WKB approximation; and second, with regard to the validity of the global amplitude balance model of Lindzen (1981) as a "saturation" criterion in the GDC model. On both counts the numerical model results have seemed quite predictable. Because in the GDC model the WKB approximation is invoked in time and height, violations of this approximation in either dimension will produce non-WKB effects, notably critical layer spreading and partial reflection.

Section V has introduced a convective adjustment parameterization which is intended to serve as a local, multi-dimensional generalization of Lindzen's (1981) one-dimensional global amplitude balance model. The simple case studies presented here, in which a single Fourier harmonic interacts with the mean flow in the vicinity of its critical level, seem to confirm the underlying assumption of Lindzen's (1981) model, viz that convective instabilities primarily act to restrain the amplitude of the overturning wave so as to prevent further overturning. Perhaps the reason for this agreement is largely geometrical; the difference between Lindzen's neutral single wave and the neutral configuration returned by our convective adjustment scheme is, after all, not great.

These case studies are of somewhat limited interest due to their simplicity, but perhaps the most significant feature of our local convective adjustment scheme is its applicability to more complex wave, mean-flow profiles. It is to these more interesting, multi-harmonic case studies that our attention will turn in the coming years. Moreover, the transient development of the nonlinear solutions has not yet been addressed here, but the turbulence parameterization introduced in Section V will enable us to determine whether or not, or under what circumstances, these solutions are attainable, and if nonlinear reflection is important.

## References

Andrews, D.G. and M.E. McIntyre, 1976: "Planetary waves in horizontal and vertical shear: the generalized Eliassen-Palm relation and the mean zonal acceleration," J. Atmos. Sci., 33, 2031-2048.

Andrews, D.G. and M.E. McIntyre, 1978: "An exact theory of nonlinear waves on a Lagrangian mean flow," J. Fluid Mech., 89, 609-646.

Baker, G.R., D.I. Meiron, and S.A. Orszag, 1982: "Generalized vortex methods for free-surface flow problems," J. Fluid Mech., 123, 477-501.

Balachandran, N.K., 1980: "Gravity waves from thunderstorms," Mon. Wea. Rev., 108, 804-816.

Balsley, B.B., W.L. Ecklund, D.A. Carter, and P.E. Johnston, 1980: "The MST radar at Poker Flat, Alaska," Radio Sci., 15, 213-223.

Balsley, B.B., and K.S. Gage, 1980: "The MST radar technique: potential for middle atmosphere studies," Pure and Appl. Geophys., 118, 452-493.

Balsley, B.B. W.L. Ecklund, and D.C. Fritts, 1983: "VHF echoes from the high-latitude mesosphere and lower thermosphere: observations and interpretations," J. Atmos. Sci.

Beland, M., 1978: "The evolution of a nonlinear Rossby wave critical level: effects of viscosity," J. Atmos. Sci., 35, 1802-1815.

Benney, D.J. and R.F. Bergeron, 1969: "A new class of nonlinear waves in parallel flows," Stud. Appl. Math., 48, 181-204.

Blumen, W. and S.C. Dietze, 1981: "An analysis of three-dimensional mountain lee waves in a stratified shear flow," J. Atmos. Sci., 38, 1949-1963.

Booker, J.R. and F.P. Bretherton, 1967: "The critical layer for internal gravity waves in a shear flow," J. Fluid Mech., 27, 513-539.

Boyd, J.P., 1976: "The noninteraction of waves with the zonally averaged flow on a spherical earth and the interrelationships of eddy fluxes of energy, heat, and momentum," J. Atmos. Sci., 33, 2285-2291.

Bretherton, F.P., 1966: "The propagation of groups of internal gravity waves in a shear flow," Quart. J. Roy. Meteor. Soc., 92, 446-480.

Bretherton, F.P. and C.J.R. Garrett, 1968: "Wavetrains in inhomogeneous moving media," Proc. Roy. Soc. London, A302, 529-554.

Brown, S.N. and K. Stewartson, 1980: "On the nonlinear reflexion of a gravity wave at a critical level. Part 1," J. Fluid Mech., 100, 577-596.

Charney, J.G. and P.G. Drazin, 1961: "Propagation of planetary scale disturbances from the lower into the upper atmosphere," J. Geophys. Res., 66, 83-109.

Coy, L., 1983: "A slowly varying model of gravity wave, mean-flow interaction in a compressible atmosphere," J. Atmos. Sci.

Curry, M.J. and R.C. Murty, 1974: "Thunderstorm-generated gravity waves," J. Atmos. Sci., 31, 1402-1408.

Davis, R.E., 1969: "On the high Reynolds number flow over a wavy boundary," J. Fluid Mech., 36, 337-346.

Davis, P.A. and W.R. Peltier, 1979: "Some characteristics of the Kelvin-Helmholtz and resonant overreflection modes of shear flow instability and their interaction through vortex pairing," J. Atmos. Sci., 36, 2394-2412.

Drazin, P. and W. Reid, 1981: Hydrodynamic Stability, Cambridge University Press, 525 pp.

Dunkerton, T.J., 1980: "A Lagrangian mean theory of wave, mean-flow interaction with applications to nonacceleration and its breakdown," Rev. Geophys. Space Phys., 18, 387-400.

Dunkerton, T.J., 1981: "Wave transience in a compressible atmosphere, part 1: transient internal wave, mean-flow interaction," J. Atmos. Sci., 38, 281-297.

Dunkerton, T.J., 1982a: "Wave transience in a compressible atmosphere part 3: the saturation of internal gravity waves in the mesosphere," J. Atmos. Sci., 39, 1042-1051.

Dunkerton, T.J., 1982b: "Stochastic parameterization of gravity wave stresses," J. Atmos. Sci., 39, 1711-1725.

Duran, D.R. and J.B. Klemp, 1982: "The effects of moisture on trapped mountain lee waves," J. Atmos. Sci., 39, 2490-2506.

Eliassen, A. and E. Palm, 1960: "On the transfer of energy in stationary mountain waves," Geophys. Publ., 22 No. 3.

Fritts, D.C., 1979: "The excitation of radiating waves and Kelvin-Helmholtz instabilities by the gravity wave-critical layer interaction," J. Atmos. Sci., 36, 12-23.

Fritts, D.C., 1982a: "Shear excitation of atmospheric gravity waves," J. Atmos. Sci.

Fritts, D.C., 1982b: "The transient critical-level interaction in a Boussinesq fluid," J. Geophys. Res.

Fua, D., G. Chimonas, F. Einaudi, and O. Zeman, 1982: "An analysis of wave-turbulence interaction," J. Atmos. Sci., 39, 2450-2463.

Grimshaw, R., 1975: "Nonlinear internal gravity waves and their interaction with the mean wind," J. Atmos. Sci., 32, 1779-1793.

Haberman, R., 1972: "Critical layers in parallel flows," Stud. Appl. Math., 51, 139-160.

Holton, J.R., 1982: "The role of gravity wave-induced drag and diffusion in the momentum budget of the mesosphere," J. Atmos. Sci., 39, 791-799.

Jones, W.L. and D.D. Houghton, 1971: "The coupling of momentum between internal gravity waves and mean flow: a numerical study," J. Atmos. Sci., 28, 604-608.

Klemp, J.B. and D.K. Lilly, 1978: "Numerical simulation of hydrostatic mountain waves," J. Atmos. Sci., 35, 78-107.

Koop, C.G., 1981: "A preliminary investigation of the interaction of internal gravity waves with a steady shearing motion," J. Fluid Mech.

Lalas, D.P. and F. Einaudi, 1976: "On characteristics of gravity waves generated by atmospheric shear layers," J. Atmos. Sci., 33, 1248-1259.

Larsen, M.F., W.E. Swartz, and R.F. Woodman, 1982: "Gravity wave generation by thunderstorms observed with a vertically-pointing 430 MHz radar," Geophys. Res. Lett., 9, 571-574.

Leovy, C.B., 1964: "Simple models of thermally driven mesospheric circulations," J. Atmos. Sci., 21, 327-341.

Lindzen, R.S., 1981: "Turbulence and stress due to gravity wave and tidal breakdown," J. Geophys. Res., 86C, 9707-9714.

Lindzen, R.S. and J. Forbes, 1983: "Turbulence originating from convectively stable internal waves," J. Geophys. Res..

Lindzen, R.S. and A.J. Rosenthal, 1976: "On the instability of Helmholtz velocity profiles in stably stratified fluids when a lower boundary is present," J. Geophys. Res., 81, 1561-1571.

Lindzen, R.S. and M.R. Schoeberl, 1982: "A note on the limits of Rossby wave amplitudes," J. Atmos. Sci., 39, 1171-1174.

Mahlman, J.D. and R.W. Sinclair, 1979: "Recent results from the GFDL troposphere-stratosphere-mesosphere general circulation model," IUGG-IAMAP XVII General Assembly, Canberra, Australia.

Maslowe, S.A., 1973: "Finite-amplitude Kelvin-Helmholtz billows," Boundary-Layer Meteor., 5, 43-52.

Maslowe, S.A., 1977: "Weakly nonlinear stability theory of stratified shear flows," Quart. J. Roy. Met. Soc., 103, 769-783.

Matsuno, T., 1982: "A quasi one-dimensional model of the middle atmosphere circulation interacting with internal gravity waves," J. Meteor. Soc. Japan, 60, 215-226.

McComas, C.H. and F.P. Bretherton, 1977: "Resonant interaction of oceanic internal waves," J. Geophys. Res., 82, 1397-1412.

McIntyre, M.E. and M.A. Weissman, 1978: "On radiating instabilities and resonant overreflection," J. Atmos. Sci., 35, 1190-1196.

Orlanski, I. and K. Bryan, 1969: "Formation of the thermocline step structure by large-amplitude internal gravity waves," J. Geophys. Res., 74, 6975-6983.

Orlanski, I. and B.B. Ross, 1973: "Numerical simulation of the generation and breaking of internal gravity waves," J. Geophys. Res., 78, 8808-8826.

Patnaik, P.D., F.S. Sherman, and G.M. Corcos, 1976: "A numerical simulation of Kelvin-Helmholtz waves of finite amplitude," J. Fluid Mech., 73, 215-240.

Peltier, W.R. and T.L. Clark, 1979: "The evolution and stability of finite amplitude mountain waves," J. Atmos. Sci., 36, 1498-1529.

Salby, M.L., D.L. Hartmann, P.L. Bailey, and J.C. Gille, 1983: "Evidence for equatorial Kelvin modes in Nimbus 7 LIMS."

Thorpe, S.A., 1981: "An experimental study of critical layers," J. Fluid Mech., 103, 321-344.

Vincent, R.A. and I.M. Reid, 1983: "HF Doppler measurements of mesospheric gravity wave momentum fluxes," J. Atmos. Sci.

Warn, T. and H. Warn, 1978: "The evolution of a nonlinear Rossby wave critical level," Stud. Appl. Math., 59, 37-71.

Weinstock, J., 1982: "Nonlinear theory of gravity waves: momentum deposition, generalized Rayleigh friction, and diffusion," J. Atmos. Sci., 39, 1698-1710.

PUBLICATION LIST FOR  
TIMOTHY J. DUNKERTON

1. Stanford, J. L., and T. J. Dunkerton, 1977: The character of ultra-long stratospheric temperature waves during the 1973 Austral winter. Beitrage zur Physik der Atmosphare, 51, 174-188.
2. Holton, J. R., and T. J. Dunkerton, 1978: On the role of wave transience and dissipation in stratospheric mean flow vacillations. J. Atmos. Sci., 35, 740-744.
3. Dunkerton, T. J., 1978: On the mean meridional mass motions of the stratosphere and mesosphere. J. Atmos. Sci., 35, 2325-2333.
4. \_\_\_\_\_, 1979: On the role of the Kelvin wave in the westerly phase of the semiannual zonal wind oscillation. J. Atmos. Sci., 36, 32-41.
5. \_\_\_\_\_, 1980: A Lagrangian mean theory of wave, mean-flow interaction with applications to nonacceleration and its breakdown. Rev. Geophys. Space Phys., 18, 387-400.
6. \_\_\_\_\_, 1981: Wave transience in a compressible atmosphere, Part I: transient internal wave, mean-flow interaction. J. Atmos. Sci., 38, 281-297.
7. \_\_\_\_\_, 1981: Wave transience in a compressible atmosphere, Part II: transient equatorial waves in the quasi-biennial oscillation. J. Atmos. Sci., 38, 298-307.
8. \_\_\_\_\_, C.P.F. Hsu, and M. E. McIntyre, 1981: Some Eulerian and Lagrangian diagnostics for a model stratospheric warming. J. Atmos. Sci., 38, 819-843.
9. Dunkerton, T. J., 1981: On the inertial stability of the equatorial middle atmosphere. J. Atmos. Sci., 38, 2354-2364.
10. \_\_\_\_\_, 1982: Curvature diminution in equatorial wave, mean-flow interaction. J. Atmos. Sci., 39, 182-186.
11. \_\_\_\_\_, 1982: Shear zone asymmetry in the observed and simulated quasi-biennial oscillations. J. Atmos. Sci., 39, 461-469.
12. \_\_\_\_\_, 1982: Wave transience in a compressible atmosphere, Part III: the saturation of internal gravity waves in the mesopause. J. Atmos. Sci., 39, 1042-1051.
13. \_\_\_\_\_, 1982: The double-diffusive modes of symmetric instability on an equatorial beta-plane. J. Atmos. Sci., 39, 1653-1657.

14. \_\_\_\_\_, 1982: Stochastic parameterization of gravity wave stresses. J. Atmos. Sci., 39, 1711-1725.
15. \_\_\_\_\_, 1982: Theory of the mesopause semiannual oscillation. J. Atmos. Sci., 39, 2682-2690.
16. \_\_\_\_\_, 1983: The evolution of latitudinal shear in Rossby-gravity wave, mean-flow interaction. J. Geophys. Res., 88, 3836-3842.
17. \_\_\_\_\_, 1983: A nonsymmetric equatorial inertial instability, J. Atmos. Sci., 40, 807-813.
18. \_\_\_\_\_, 1983: Laterally-propagating Rossby waves in the easterly acceleration phase of the quasi-biennial oscillation. Atmos-Ocean., 55-68.
19. \_\_\_\_\_, 1983: Modification of stratospheric circulation by trace constituent changes? J. Geophys. Res., 88, 10831-10836.
20. \_\_\_\_\_, 1983: On the conservation of pseudoenergy in Lagrangian time mean flow. J. Atmos. Sci., 40, 2623-2629.
21. \_\_\_\_\_, and D.C. Fritts, 1984: The transient gravity wave critical layer, part I: Convective adjustment and the mean zonal acceleration. J. Atmos. Sci., (to appear).
22. \_\_\_\_\_, and N. Butchart, 1984: Propagation and selective transmission of internal gravity waves in a sudden warming. J. Atmos. Sci., (to appear).
23. Fritts, D.C., and T.J. Dunkerton, 1984: Fluxes of heat and constituents due to convectively unstable gravity waves. J. Atmos. Sci., (submitted).
24. \_\_\_\_\_, and \_\_\_\_\_, 1984: A quasi-linear study of gravity wave saturation and self-acceleration. J. Atmos. Sci., (submitted).
25. Dunkerton, T.J., 1984: Inertia-gravity waves in the stratosphere. J. Atmos. Sci., (submitted).
26. \_\_\_\_\_, and D.P. Delisi, 1984: Climatology of the equatorial lower stratosphere: An observational study. J. Atmos. Sci., (submitted).